Vol. 89: 61–83, 2022
https://doi.org/10.3354/cr01707

CLIMATE RESEARCH
Clim Res

Published online December 22

Sensitivity of precipitation and atmospheric low-level circulation patterns to domain size and choice of parameterization schemes in RegCM4.4 over Central America

Erick R. Rivera[1,2,*], Jorge A. Amador[1,2], Fernán Sáenz[2]

[1]School of Physics, University of Costa Rica, San José 11501-2060, Costa Rica
[2]Center for Geophysical Research, University of Costa Rica, San José 11501-2060, Costa Rica

ABSTRACT: The sensitivity of regional climate model simulations to domain size and position is becoming increasingly important for generating reliable climate scenarios. In this study, the Central America CORDEX domain (CCA) at 50 km horizontal resolution with a relaxation zone of 10° around the boundaries (CCA+) was taken as the basis to increase domain size in the RegCM4.4 model. The low-level circulation and precipitation patterns over Central America, the western Caribbean Sea, and the eastern tropical Pacific do not show strong sensitivity to domain size changes for an area increment of 18, 32, and 52% with respect to the size of CCA+. The physical configuration in RegCM4.4 has a greater impact on the representation of relevant climate characteristics and atmospheric processes. Simulated 925 hPa winds over the Caribbean low-level jet (CLLJ) region show unrealistic winter and summer intensities, especially in July. Similar issues were found in other studies for the CCA domain, using different models and physical configurations. A reduction of the critical Richardson number in the selected planetary boundary layer scheme resulted in little change in the strength of the summer component of the CLLJ. The model simulations do not completely capture key regional precipitation patterns such as the mid-summer drought, due to limitations in adequately representing low-level circulation. However, simulations using the Grell cumulus parameterization perform relatively better than those using a mixed scheme (Grell over land–Emanuel over ocean).

KEY WORDS: Regional climate model · Model sensitivity · Domain size · Parameterizations · CORDEX Central America · RegCM

1. INTRODUCTION

Central America and Mexico (CAM) are vulnerable to extreme weather and climate events that lead to prominent socioeconomic impacts (Amador 2011, Amador & Arce-Fernández 2022). In Central America during 2002–2012, about 2000 deaths and losses of >US$4 billion were caused by tropical cyclone activity and other hydrometeorological events (Amador & Alfaro 2014). For many years, this region has been an area of interest to scientists studying tropical cyclones (Gray 1979, Gray et al. 1992, Landsea 1993, 2005, Arce-Fernández & Amador 2021), the Intertropical Convergence Zone (ITCZ; Hastenrath 1967, Hayes et al. 1989), convective complexes (Velasco & Fritsch 1987, Feng et al. 2021, Moron & Robertson 2021, Takahashi et al. 2021), the mid-summer drought (MSD; Magaña et al. 1999), the Western Hemisphere warm pools (Wang & Enfield 2001, 2003), and the Caribbean low-level jet

*Corresponding author: erick.rivera@ucr.ac.cr

Publisher: Inter-Research · www.int-res.com

(CLLJ; Amador 1998, 2008, Hidalgo et al. 2015, Amador et al. 2016a,b). The latter system is a recognized conveyor of moisture into Central America and the mid-latitudes (Mo et al. 2005, Cook & Vizy 2010, Durán-Quesada et al. 2010, 2017, Taylor et al. 2013). All the above atmospheric phenomena largely control regional precipitation variability at different temporal and spatial scales. Intraseasonal modes strongly influence the distribution of precipitation and act as a seed for other tropical disturbances (Serra et al. 2014). On larger temporal scales, Central America is a 'hot spot' for climate impacts (Giorgi 2006, Diffenbaugh & Giorgi 2012), and is one of the most vulnerable regions in the world to climate change. Some of these impacts have already been identified in Central America; for instance, human health effects of climate change (Patz & Kovats 2002), warmer and drier growing seasons (Stewart et al. 2022), and land in Central America becoming less suitable for coffee cultivation (Lara-Estrada et al. 2021). This multiscale interaction constitutes a relevant modern scientific problem that needs to be addressed.

Regarding data availability for research and impact studies, the observational upper-air network in Central America has deteriorated extensively during the last 3 decades, leaving a tremendous knowledge gap for studies and prevention activities (Stickler et al. 2010). Conveniently, global data sets, including the National Centers for Environmental Prediction–National Center for Atmospheric Research (NCEP-NCAR) reanalysis (Kalnay et al. 1996), the European Centre for Medium-Range Weather Forecasts (ECMWF) Interim (ERA-Interim; Dee et al. 2011) data, and the ECMWF reanalysis version 5 (ERA5; Hersbach et al. 2020), supply information, regardless of their resolution, for research opportunities in regions with scarce surface and upper-air data such as Central America. Additionally, initiatives such as the Coordinated Regional Climate Downscaling Experiment (CORDEX; https://cordex.org) provide state-of-the-art numerical tools to study physical and dynamical processes at regional scales. In this work, the above data and tools are used to evaluate the sensitivity of the International Centre for Theoretical Physics (ICTP)'s Regional Climate Model (RegCM) to configuration changes over the CORDEX Central America (CCA) domain.

Coarse-resolution global circulation models (GCMs), using grid sizes of the order of 100 km or more, have a relatively poor representation of CAM climate features (Rivera & Amador 2008, Hidalgo & Alfaro 2015). Therefore, dynamical downscaling techniques and the use of regional climate models (RCMs) are useful alternatives to approach the problem of modeling regional climate variability and climate change. The sensitivity of RCM simulations to domain size and position is becoming increasingly important for generating reliable climate scenarios (Seth & Giorgi 1998, Vannitsem & Chomé 2005, Martínez-Castro et al. 2006, Leduc & Laprise 2009, Bhaskaran et al. 2012, Vichot-Llano et al. 2014, Centella-Artola et al. 2015, Suga et al. 2021, Yu et al. 2022). For example, Suga et al. (2021) performed 10 yr simulations over central and eastern Europe to study sensitivity to domain size, using the Max Planck Institute (MPI) Regional Model (REMO). The authors tested 3 different domains embedded in each other with a constant resolution of about 10 km and found that the smallest precipitation biases occurred on the largest domain. Furthermore, one important issue in the regional modeling framework is the choice of the initial conditions. In some cases, more than one driving GCM would be required due to uncertainties related to the performance of different global models (Vichot-Llano et al. 2022, Yu et al. 2022).

This work addresses the problem of domain size and location by changing, in a systematic way, the north–south, east–west, and overall extension of the CCA domain to study the sensitivity of the modeled precipitation and low-level circulations to those changes. Low-level circulations, such as the CLLJ (Amador 1998, 2008), are crucial for moisture transport in the region (Mo et al. 2005, Durán-Quesada et al. 2010, 2017, Gimeno et al. 2016) and influence the precipitation distribution through their interactions with other climate patterns, such as El Niño–Southern Oscillation (ENSO; Amador 2008).

The experimental setup applied here also includes the use of different cumulus parameterizations and explores the effect of modifying physical parameters that control some characteristics of the modeled planetary boundary layer (PBL). The CCA region is characterized by the existence of a very strong vertical wind shear associated with the CLLJ, especially in the PBL, that in many cases prevents the development of convective activity. The CLLJ's seasonal and intraseasonal changes would be expected to provide different conditions in the PBL, which can impact convection and eddy energy as well as moisture transport above the ocean surface.

Past studies have addressed the importance of statistical and dynamical downscaling tools applied to weather and climate in Central America (e.g. Amador 2008, Amador & Alfaro 2009). Rivera & Amador (2008, 2009) evaluated the representation of relevant cli-

mate characteristics of Central America in 2 GCMs: the ECMWF Hamburg Model version 4.5 (ECHAM4.5) and the Community Climate Model version 3.6 (CCM3.6). For the period 1990–1999, the former model more realistically represented the regional precipitation and low-level wind fields. Dynamical downscaling of ECHAM4.5 simulations for January 2000, using the fifth-generation Mesoscale Model (MM5) version 3 (MM5v3) at 30 km resolution, showed that the regional model properly simulated the position of the CLLJ, but its intensity was underestimated by 1–3 m s^{-1}. Regarding the precipitation spatial patterns, MM5v3 agreed reasonably well with observations and satellite estimations (i.e. drier areas in the Pacific, wetter areas in the Caribbean). Nonetheless, rainfall accumulations were overestimated.

Later, Karmalkar et al. (2011) showed that the Providing Regional Climates for Impacts Studies (PRECIS) model, driven by the third-generation Hadley Centre Atmospheric Model (HadAM3P), adequately captured the spatial distribution of precipitation in Central America, although there was a precipitation bias of −30% (21%) in the wet (dry) season. On the other hand, the structure, intensity, and seasonal variation of the CLLJ was well-simulated by this regional model using a 0.22 × 0.22° horizontal grid. Centella-Artola et al. (2015) reported sensitivity of PRECIS-simulated CLLJ and MSD to domain position for grid spacings of about 50 km. The above 2 results exemplify to some extent the value of a higher horizontal resolution in the models. However, it does not account for the discrepancy and bias in the precipitation distribution, suggesting that both the PBL and cumulus parameterizations may also play a role in determining the CLLJ position and associated rainfall patterns.

Diro et al. (2012) performed simulations for the period 1997–2003 over the CCA domain, using RegCM4. The model simulations represented the annual cycle and spatial distribution of precipitation over CAM, as well as the connection between enhanced CLLJ intensity and the occurrence of the MSD. Nonetheless, they exhibited a weaker and southerly displaced CLLJ. In addition, sensitivity experiments showed that RegCM4 runs using the Community Land Model (CLM) simulated less seasonal rainfall over land than the control run (using the Biosphere–Atmosphere Transfer Scheme; BATS).

RegCM4 simulations for 1998–2003, under different cumulus parameterization schemes (Emanuel, Grell over land–Emanuel over ocean, and Tiedtke with tuned parameter values), were carried out by Martínez-Castro et al. (2018). These model runs captured the observed monthly mean spatial distributions of temperature and precipitation over land areas of Central America and the Caribbean. However, large precipitation biases (>7 mm d^{-1}) occurred during the rainy season at some locations. On the other hand, the representation of the CLLJ in the model simulations was more intense (less intense) during the boreal winter (summer) for some physical configurations.

Martínez et al. (2019) argued that wet biases over land areas of Central America and northern South America in a climatology (1982–2012) from the Weather Research and Forecasting (WRF) model are linked to excessive moisture convergence. These authors suggest that regional precipitation biases are determined not only by the cumulus parameterization schemes but also by simulated circulation patterns. In this regard, the CLLJ intensity in WRF was stronger than with ERA-Interim.

Historical CCA simulations, using REMO and the coupled REMO-MPI Ocean Model system (ROM), were performed by Cabos et al. (2019). Both models were forced by ERA-Interim and the MPI Earth System Model (MPI-ESM). Compared to REMO, the ROM model improved representation of the ITCZ and CLLJ. In terms of precipitation, the coupled model simulations better captured the MSD as well as the seasonal cycle and spatial distribution of precipitation, particularly in southern Central America.

A coupled ocean–atmosphere climate simulation over Central America, using the Regional Spectral Model-Regional Ocean Model System (RSM-ROMS), was reported by Misra & Jayasankar (2022). The initial and lateral boundary conditions of the atmosphere were provided by the NCEP-Department of Energy (NCEP-DOE) reanalysis. This model system correctly simulated the seasonal cycles of the CLLJ and precipitation over land, including the MSD. However, the annual mean low-level wind magnitude in the CLLJ region was underestimated, and simulated precipitation showed a significant wet bias over the Central American isthmus. Added value with respect to the driving reanalysis was obtained for low-level winds but not for precipitation distribution.

Table 1 summarizes some of the major findings of the above studies that are relevant to this work, with emphasis on the ability of several RCMs to simulate the regional precipitation characteristics and the position and intensity of the CLLJ. In general, models and model configurations applied so far are distinct from each other, especially in the data for model ini-

Table 1. Key model configurations and results from previous studies; see Section 1 for model abbreviations and acronyms

Authors	GCM/RCM (grid spacing in parenthesis)	PBL/cumulus schemes in RCM	CLLJ intensity/ position	Precipitation totals/ distribution in Central America
Rivera & Amador (2009)	ECHAM4.5 (2.8°)/ MM5v3 (0.25°)	MRF/Grell and Kain-Fritsch	Undervalued/Good	Undervalued/ Drier (wetter) Pacific (Caribbean)
Karmalkar et al. (2011)	HadAM3P (3.75 × 2.5°)/PRECIS (0.22°)	Physical package of HadAM3P[a]	Good/Good	Negative (positive) bias in the wet (dry) season/Spatial distribution well simulated
Diro et al. (2012)	ERA-Interim (1.5°)/ RegCM4 (0.5°)	Holtslag/Emanuel (ocean)–Grell (land)	Underestimated, stronger in CLM/ Displaced to the south	CLM: less rain over land as compared to BATS/Negative correlation with CLLJ
Centella-Artola et al. (2015)	ERA-Interim (1.5°)/ PRECIS (0.44–0.22°)	Physical package of HadAM3P[a]	Sensitivity to domain size	Good, but depends on domain configuration
Martínez-Castro et al. (2018)	ERA-Interim (1.5°)/ RegCM4 (0.22°)	Holtslag/Emanuel, Emanuel (ocean)–Grell (land) and Tiedtke	Stronger (weaker) during winter (summer)/Extended during winter	Greater biases in the rainy season/Well represented over land
Martínez et al. (2019)	ERA-Interim (0.75°)/ WRF (0.22°)	Mellor-Yamada-Janjic/Kain-Fritsch	Stronger than ERA-Interim	Positive biases over land
Cabos et al. (2019)	ERA-Interim (0.75°) and MPI-ESM (1.9°)/ REMO and ROM (0.44–0.22°)	Physical package of ECHAM4	Improved representation in coupled simulations	Reduced precipitation bias in coupled runs/ Good representation
Misra & Jayasankar (2022)	NCEP-DOE (2.0°)/ RSM-ROMS (15 km)	Hong-Pan/ Moorthi-Suarez	Weaker intensity/ Reasonable	Wet bias over land

[a]The convective scheme is the mass flux penetrative scheme with an explicit downdraft (Gregory & Rowntree 1990)

tialization, the spatial resolutions, and the cumulus schemes used. Some additional works, using configurations other than those in Table 1, have also failed to reproduce the July peak of the CLLJ (Vichot-Llano et al. 2022 and references therein).

The CLLJ is a regional climate feature that has not been captured well enough to account for its connection with the precipitation distribution, as proposed by Hidalgo et al. (2015). Based on a literature review, the current work is unprecedented in terms of considerations of domain size, cumulus parameterizations, and changes in the boundary layer depth in the CAM region. The results shown in Table 1, added to the outcome of this work, will hopefully enhance the understanding of the low-level circulation (i.e. CLLJ) and associated precipitation patterns in this region.

2. MATERIALS AND METHODS

2.1. Data and model configuration

The climate model used here is version 4.4 of the ICTP RegCM model (RegCM4.4; Giorgi et al. 2014). RegCM4.4 incorporates the hydrostatic dynamical core of MM5 in a sigma coordinate system framework. All regional model simulations presented in this work were driven by 0.75° resolution ERA-Interim 6-hourly data starting on 1 January 2005 (at 00:00 h UTC) and run continuously for 7 yr until 1 January 2012 (at 00:00 h UTC). The first year was excluded from the analysis to allow the model to spin-up. Sea surface temperature (SST) fields were obtained from the National Oceanic and Atmospheric Administration (NOAA) Weekly Optimum Interpolation SST (OISST) data set.

As in Diro et al. (2012), the RegCM4.4 model uses the following physical parameterizations: (1) the microphysics scheme of Pal et al. (2000), (2) BATS (Dickinson et al. 1993) to represent land surface processes, (3) the CCM3 radiation scheme (Kiehl et al. 1996), and (4) the Holtslag et al. (1990) boundary layer representation, hereafter referred to as Holtslag.

2.2. Model sensitivity experiments

The CAM region is influenced by multiple climate signals, and few major modeling studies have been reported for the region so far (see, for example, Table 1). Dynamic interaction on the meso–beta scales is unknown (Amador 2008). An example of this lack of knowledge is the interaction of easterly waves with the CLLJ during the rainy season, which is also true for longer temporal and spatial scales.

The CLLJ has a zonal extent of more than 2500 km and a meridional range of circa 500 km, while the MSD is a phenomenon covering parts of the eastern tropical Pacific (ETP), from southwestern Mexico to Costa Rica and Panama. The correct simulation of the regional circulation at medium horizontal scales (25–50 km) is then fundamental for a realistic representation of convective activity and precipitation. In this respect, the CLLJ is considered an important dynamical mechanism associated with the regional rainfall distribution at different temporal and spatial scales (e.g. Mora et al. 2020 for sea breeze, Amador & Arce-Fernández 2022 for regional lightning densities). Therefore, the CCA domain at 50 km (0.44°) horizontal resolution and 18 sigma vertical levels (model top at 50 hPa), with a relaxation zone of 10° around the boundaries (CCA+) is the basis to increase domain size in the RegCM4.4 model. Diro et al. (2012) and Martínez-Castro et al. (2018) also used this vertical resolution for their climate simulations over the CCA region.

The objective here is to test the sensitivity of the precipitation distribution and its basic statistical attributes and the atmospheric low-level circulation patterns within CCA to changes in domain size and parameterization schemes in the RegCM4.4 model. The modifications in the domain configuration are useful to assess if the specified CCA domain has the correct initial boundary information so that all winter and summer processes affecting the Central American region can be well-represented by the regional model. A domain that is too small, for example, could limit the ability of the regional model to adequately capture cold air intrusions during the boreal winter or the propagation of easterly waves during the warm season.

2.2.1. Fixed physics configuration

By initially setting a fixed physics configuration in RegCM4.4, the CCA+ domain size is changed in steps of a Delta (Δ) of 10° in the following manner: (1) increase of 1 Δ in all model boundaries (CCA+ALL); (2) increase of 1 Δ in each of the northern and southern model boundaries only (CCA+NS); and (3) increase of 1 Δ in both the eastern and western model boundaries only (CCA+EW). Fig. 1a shows the above domain configurations. The ratios of the CCA+EW, CCA+NS, and CCA+ALL domain areas to the CCA+ domain (the control domain [CTL]) are 118, 132, and 152%, respectively. These changes in the domain of the model simulations go from a small portion of the CCA area to more than 1.5 times that area, which is considered sufficient to study the sensitivity of regional precipitation and low-level circulations to domain changes. The cumulus convection parameterization of Grell (1993), with an Arakawa & Schubert (1974) closure scheme, is used for these runs ('G' experiments). The domain configuration considers both the north–south and east–west physical forcings that interact with the systems within the CCA.

2.2.2. Convective model configuration

This configuration is the same as in Section 2.2.1, except for the use of 2 convective parameterizations in each domain: Grell (1993) over land and Emanuel (1991) over ocean ('GE' experiments). These convection schemes have been used in numerical simulations performed with more recent versions of the RegCM model at horizontal resolutions equal to or higher than that of this study (see, for example, Pareja-Quispe et al. 2021, Torres-Alavez et al. 2021, Villafuerte et al. 2021, Kouassi et al. 2022, Pant et al. 2022).

2.2.3. Boundary layer experiment

Some of the studies presented in Table 1 have shown that the RegCM model underestimates the intensity of the CLLJ, particularly in summer. Weaker simulated winds at 925 hPa could be related to strong eddy diffusion of momentum within the boundary layer.

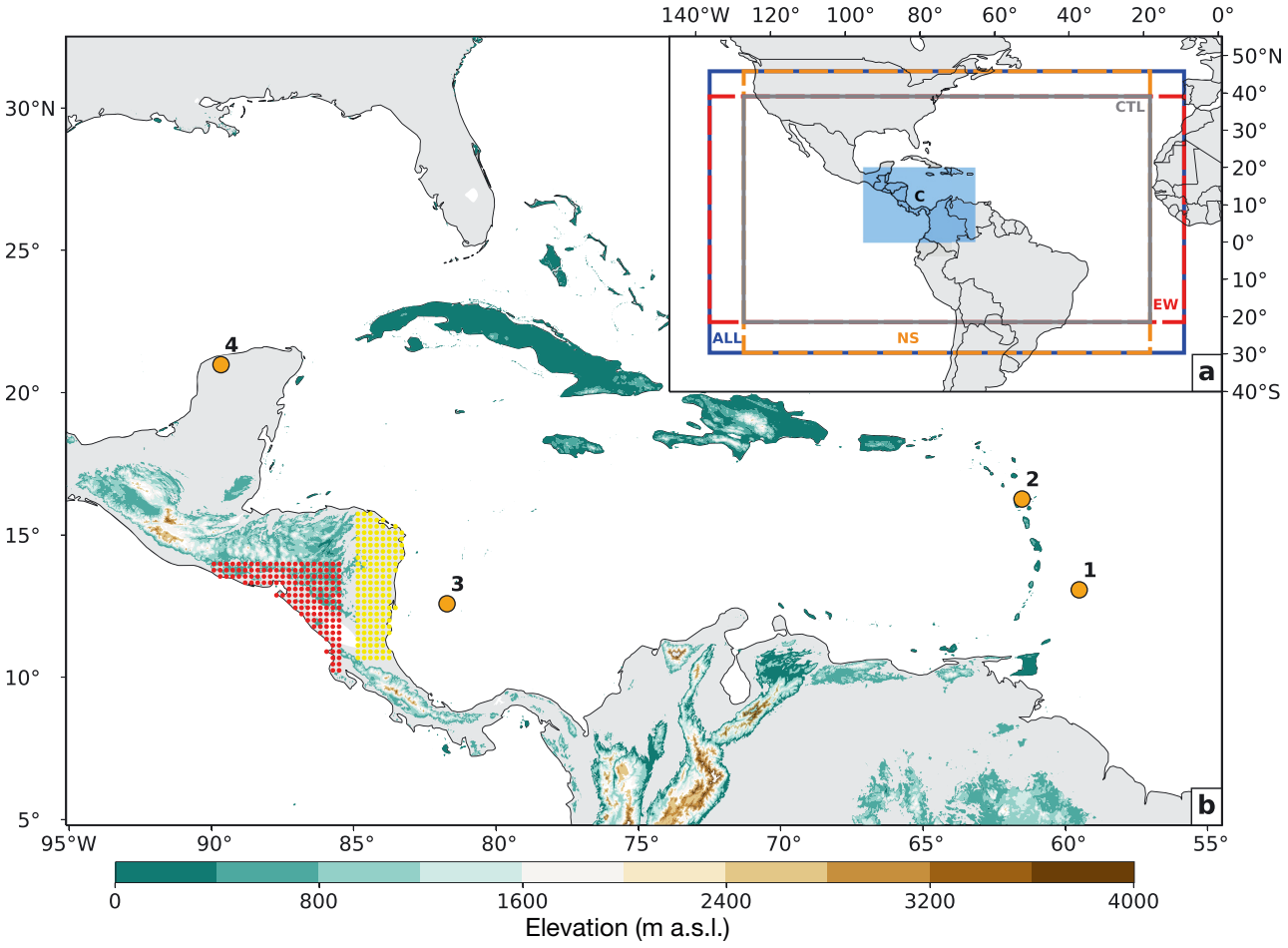

Fig. 1. (a) Representation of the 4 model domains used in this study. CTL: control run or CCA+ (grey rectangle), ALL ≈ 1.52 CTL (blue rectangle), EW ≈ 1.32 CTL (dashed red rectangle) and NS ≈ 1.18 CTL (dashed orange rectangle). The Central subdomain (C), representing Central America, the western Caribbean Sea, and the eastern tropical Pacific, corresponds to the light blue shaded area (0–20° N, 65–95° W). (b) Topographical map showing the location (orange circles) of the radiosonde stations. 1: Grantley Adams, Barbados; 2: Le Raizet, Guadeloupe; 3: San Andrés, Colombia; 4: Mérida, Mexico. Regional model grid points on the Pacific (Caribbean) side of Central America are indicated with red (yellow) stippling. See Section 2 for abbreviations and acronyms

The boundary layer height (BLH) in the Holtslag scheme is diagnosed in terms of the critical Richardson number (Ric), which means that this parameter also affects the turbulent fluxes and eddy diffusivity (Holtslag et al. 1990). A reduction of Ric decreases the BLH, as shown by Zhang et al. (2015).

This experiment is based on the hypothesis that a lower value of Ric in the RegCM4.4 model would result in a shallower boundary layer and decreased turbulent diffusion over the Caribbean Sea region. This could favor the development of a stronger CLLJ. Therefore, changes in the Holtslag PBL scheme configuration are introduced in simulations for the CCA+ALL domain to explore the model's sensitivity to reductions in this parameter. The physical parameterizations follow those in Sections 2.2.1 and 2.2.2. Two additional values of Ric are used over both land and ocean: 0.20 (which is similar to the lowest value in Zhang et al. 2015) and 0.10. By default, Ric in RegCM4.4 is equal to 0.25.

2.3. Model metrics

The RegCM4.4 results for all experiments are compared with reference fields and special climatic features of Central America and southern Mexico (e.g. the MSD). The Tropical Rainfall Measuring Mission (TRMM; Huffman et al. 2007) and the Climate Hazards Group InfraRed Precipitation with Station (CHIRPS; Funk et al. 2015) data sets are used for validating model rainfall. CHIRPS is one of the best-

performing gridded precipitation products in the Caribbean (Centella-Artola et al. 2020) and Central America (Stewart et al. 2022).

The monthly RegCM4.4 and CHIRPS precipitation during 2006–2011, averaged over the Pacific and Caribbean regions of Central America (as defined in Fig. 1b), was used to calculate the standardized precipitation index (SPI; McKee et al. 1993) for 1–24 mo accumulation periods. This serves to validate the seasonal to interannual variability of model precipitation. In this regard, the Pearson correlation between observed and modeled time series of SPI-6, SPI-12, SPI-18, and SPI-24 was obtained to determine the simulations' ability to capture the occurrence of wet and dry periods at different timescales. As conceptualized by the World Meteorological Organization (WMO 2012), an *n*-month SPI, where *n* is the number of months of accumulation, provides a comparison of the precipitation over a specific *n*-month period, with the precipitation totals from the same *n*-month period for all the years in the period of study.

Mean fields estimated from both radiosonde data (available at the University of Wyoming archive; http://weather.uwyo.edu) and ERA5 reanalysis help to test the ability of the model to capture the seasonal cycle of low-level atmospheric circulation features, such as the CLLJ. ERA5 has been used as a reference data set in previous works, some aimed at validating model simulations over the CAM region (e.g. Beck et al. 2020, García-Franco et al. 2020, Ortega et al. 2021, Yu et al. 2021, Stewart et al. 2022). Fig. 1b shows the location of the sounding sites used in this work: Grantley Adams (Barbados), Le Raizet (Guadeloupe), San Andrés (Colombia), and Mérida (Mexico). The relevance of including the CLLJ in the metrics to evaluate RegCM4.4 model performance relies on the significant role of this structure as a conveyor of moisture from the Caribbean Sea into Central America, the ETP, the Gulf of Mexico, and the North American Great Plains (Mo et al. 2005, Durán-Quesada et al. 2010, Gimeno et al. 2016).

The skill of the model simulations is evaluated in the Central (C) region (see Fig. 1a) by computing the mean bias, the spatial root mean square error (RMSE), the pattern correlation coefficient, and the spatial standard deviation. The latter 3 statistics are presented in Taylor diagrams (Taylor 2001). Following Amador (2008), the area 12.5–17.5° N, 75–80° W is defined as a CLLJ index region.

For comparison purposes, TRMM (0.25°), CHIRPS (0.05°), and ERA5 (0.25°) data, along with the RegCM4.4 simulations, were regridded to a common 0.44° grid using bilinear interpolation (same grid as in CTL, except for the boundary layer experiment where CCA+ALL was used). These simulations are also contrasted with RegCM version 4.7 (RegCM4.7) results, as described by Torres-Alavez et al. (2021), over the CLLJ index region and for the period 2006–2011.

The 95% confidence interval for the difference in means and the correlation coefficients was calculated with the bias-corrected and accelerated (BCa) bootstrap method (DelSole & Tippett 2022) using 1000 bootstrap samples.

3. RESULTS

3.1. Wind at 925 hPa

Fig. 2 presents the mean wind fields at 925 hPa for subdomain C. According to Fig. 2a, the ERA5 annual mean winds present moderate-to-large intensities (about 12 m s^{-1}) over the CLLJ region. Here, it is important to point out that the driving ERA-Interim reanalysis and ERA5 have similar low-level wind magnitudes across subdomain C and in the CLLJ index area, as shown in Figs. S1 & S2 in the Supplement at www.int-res.com/articles/suppl/c089p061_supp.pdf. Notably, the RegCM4.4 G simulations underestimate the magnitude of the annual mean low-level wind, especially over the central and western Caribbean Sea (Fig. 2b–e). All experiments under the G convection scheme produce similar results, and no dependence on the domain size is clearly identified.

The CLLJ presents 2 maxima in February and July. According to ERA5, the February 925 hPa wind magnitude reaches over 14 m s^{-1} in the western Caribbean Sea (Fig. 2f). The RegCM4.4 G simulations capture this winter maximum of the CLLJ, but wind intensities at the jet core region (around 12.5° N, 75° W) are weaker (Fig. 2g–j). In addition, the trans-isthmic Papagayo and Panama jets can also be observed in the reanalysis data (Fig. 2f,k). The gap winds appear to be exaggerated in ERA5 in February and diminished in July compared to the Cross-Calibrated Multi-Platform Ocean Surface Vector Analysis data (Amador et al. 2016a,b). This issue is particularly difficult to explain since the CLLJ reaches its maximum intensity at 925 hPa and largest tropospheric depth in July, but it could be related to changes in the meridional wind component from February to July in response to land–ocean thermal contrasts during the summer season of each hemisphere (Amador 2008). The Papagayo jet, a strong mechanism associated with the MSD and other features in the ETP (Amador & Arce-Fernández 2022), is underestimated by all simulations.

The simulated reduction of the CLLJ intensity is more evident in July. According to ERA5, wind speeds in the CLLJ region during that month are greater than 14 m s^{-1} (Fig. 2k). In the G simulations

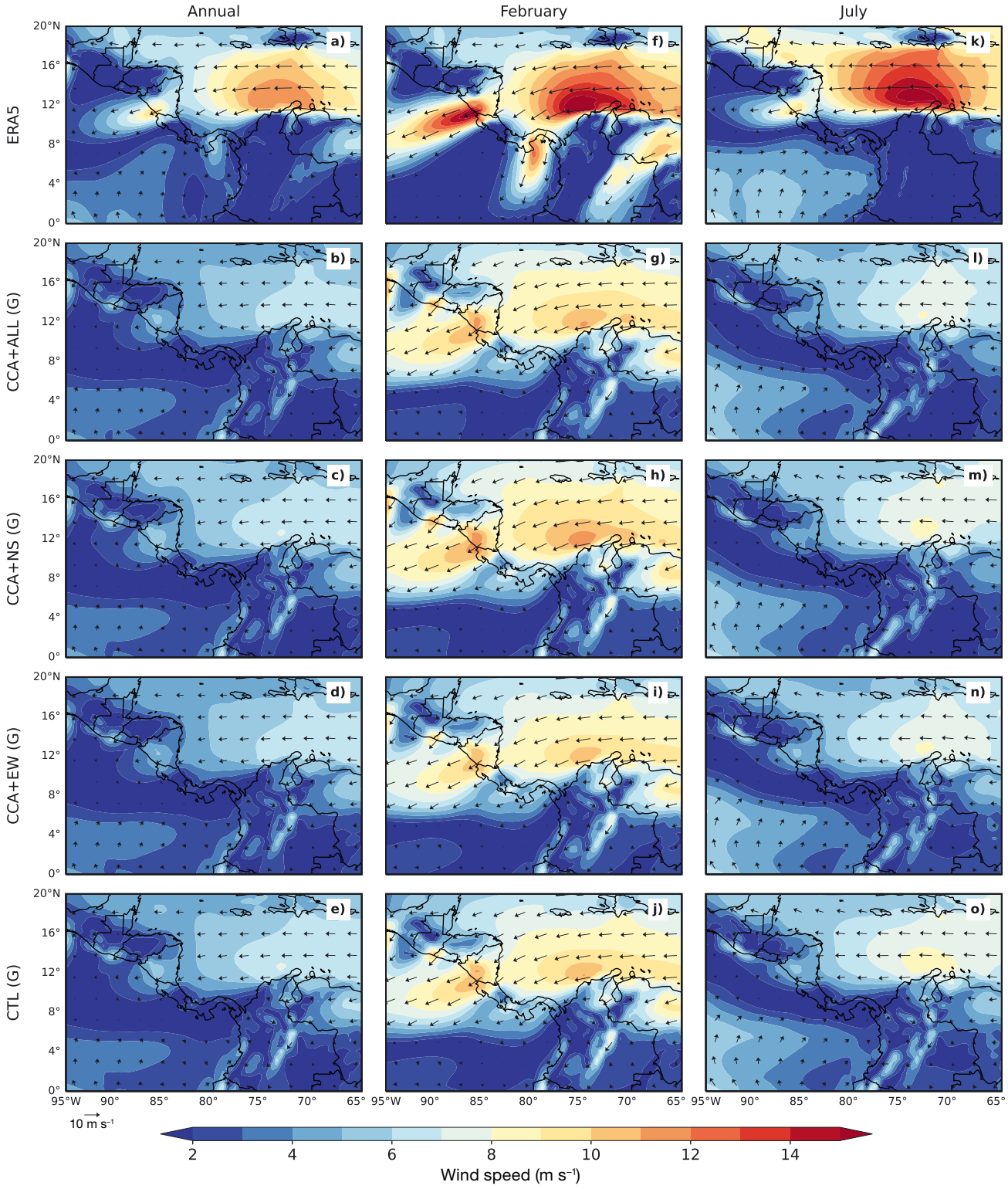

Fig. 2. Annual, February, and July mean winds at 925 hPa during 2006–2011 for (a,f,k) ERA5, and RegCM4.4 experiments using G cumulus parameterization for (b,g,f) CCA+ALL, (c,h,m) CCA+NS, (d,i,n) CCA+EW, and (e,j,o) CTL. See Sections 1 and 2 for abbreviations and acronyms

(Fig. 2l–o), the maximum wind off the east coast of Central America is less than 9 m s^{-1}. The summer CLLJ peak is slightly better represented by the CTL (CCA+) simulation (Fig. 2o). Results for February and July also show that the model's behavior is not strongly dependent on domain size, at least over Central America, the Caribbean Sea, and the ETP. A weaker CLLJ in the model simulations can have serious implications for moisture transport into Central America and the position of the ITCZ, as will be discussed in Section 3.2. Weaker gap winds than those observed in the ETP are likely to introduce large biases in the SST distribution over the Costa Rica Dome (CRD; Kessler 2006). A potential future improvement in the representation of the CLLJ may be the use of a coupled atmosphere–ocean model (see, for example, Artale et al. 2010, Cabos et al. 2019, Misra & Jayasankar 2022).

The G and GE low-level wind simulations are compared in Fig. 3. In the annual mean, the former pres-

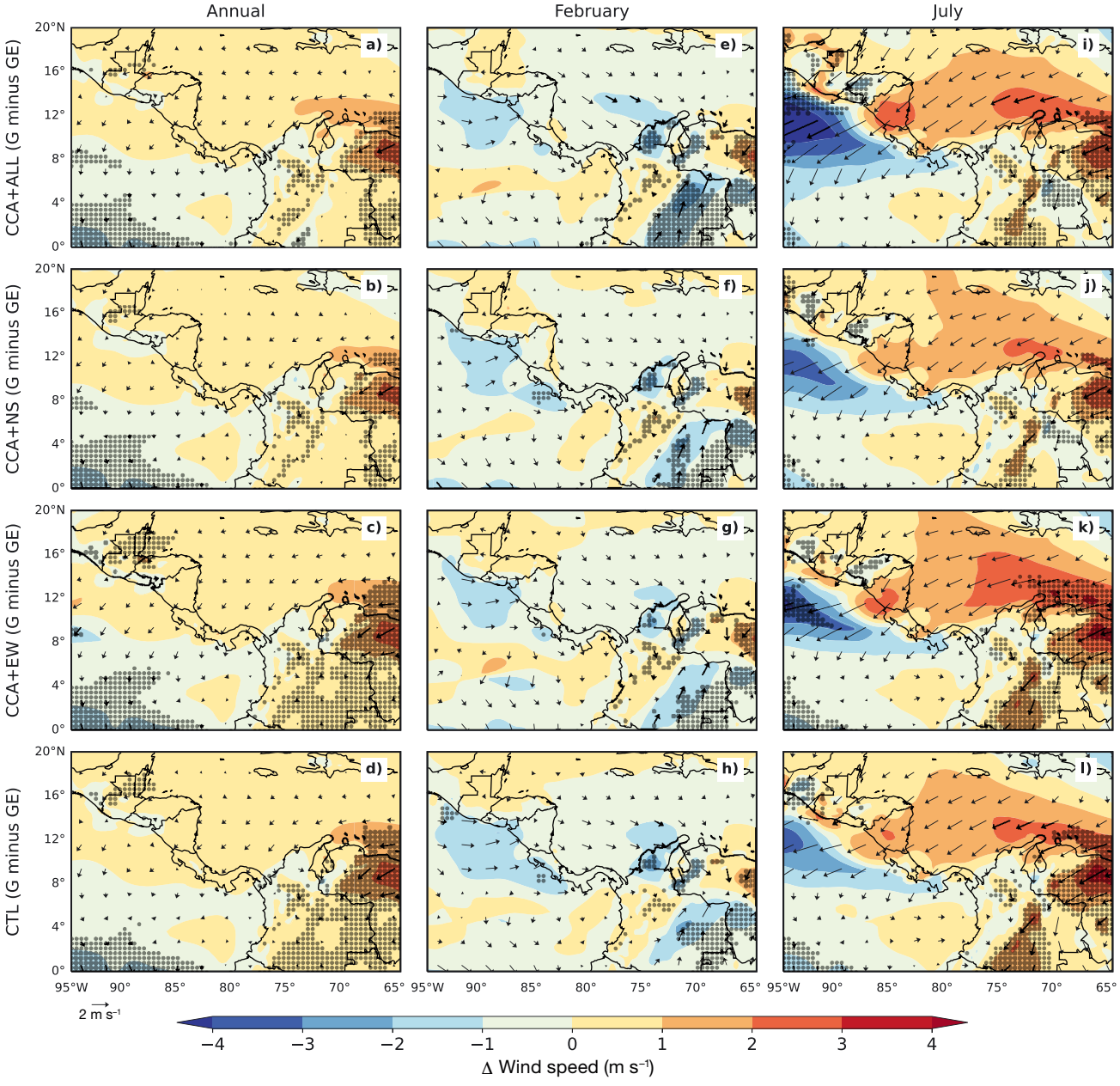

Fig. 3. Annual, February, and July mean wind difference at 925 hPa between G and GE simulations during 2006–2011 for (a,e,i) CCA+ALL, (b,f,j) CCA+NS, (c,g,k) CCA+EW, and (d,h,l) CTL. Stippled areas: statistically significant differences in wind speed at the 95% bias-corrected and accelerated confidence level. See Section 2 for abbreviations and acronyms

ents slightly stronger 925 hPa winds than the latter (Fig. 3a–d), with differences of less than 1 m s^{-1} throughout most of the CLLJ region. In February, the model runs using only the G cumulus parameterization showed weaker easterly flow over the central and western Caribbean Sea than those with the GE scheme (Fig. 3e–h), but the differences are small. In the case of July, the G simulations exceed the CLLJ intensity by more than 1 m s^{-1} compared to the GE runs (Fig. 3i–l); however, the variations are not statistically significant at the 95% BCa confidence level.

Examination of the mean annual cycle of low-level wind at RegCM4.4 grid points close to radiosonde stations across the Caribbean Sea basin and the southern Gulf of Mexico (Fig. 4) shows that both sets of model parameterization experiments (G and GE) are able to represent the observed timing of the zonal CLLJ maxima for all domain sizes, except at Barbados (Fig. 4a,b), where the boreal summer maximum in zonal wind occurs in June instead of July. The occurrence of the seasonal minima of the zonal flow over the Caribbean, as observed during March–April and September–October, is also in good agreement with model simulations for all domain sizes (Fig. 4a–f).

The intensity of the CLLJ in the zonal direction in Barbados is underestimated by the model simulations, regardless of domain size (Fig. 4a,b). In San Andrés (Fig. 4e,f), a much weaker zonal flow during the boreal summer is prominent in all experiments, but especially in those using GE. A closer agreement is present at the Guadeloupe station (Fig. 4c,d), regarding timing and intensity of seasonal extremes. In this location, however, the CLLJ zonal (meridional) flow intensity during boreal summer is weaker (stronger) in the G simulations compared with radiosonde data. In general, most of the RegCM4.4 model configurations tend to produce a diminished zonal flow in the Caribbean Sea and the southern portion of the Gulf of Mexico, particularly from May–September. Weaker low-level circulations result in less westward transport of moisture toward Central America and partially explain the negative precipitation biases in northern South America (see Section 3.2).

During the boreal winter, the modeled meridional wind does not present the correct (positive) sign in the Gulf of Mexico (see Mérida in Fig. 4g,h). This behavior can have important implications for the meridional transport of moisture to the Gulf of Mexico and southeastern North America (Mo et al. 2005), a problem that was pinpointed by Amador (2008) when comparing regional sounding station information with the NCEP-NCAR reanalysis. The negative sign of the meridional wind in Barbados (near the CLLJ entrance) for this time of year is weakly captured by the G and GE simulations for all domain sizes (Fig. 4a,b).

A comparison between the RegCM4.4 simulations from this work and those prepared by Torres-Alavez et al. (2021) using a more recent version of the model (RegCM4.7, with a 25 km grid), shows that low-level wind intensities at 925 hPa over the CLLJ index region (12.5–17.5° N, 75–80° W) are stronger in Torres-Alavez et al.'s (2021) simulations (regardless of the driving GCM), and closer to ERA5 (Fig. 5). However, the maximum of the simulated summer component of the CLLJ occurs in June instead of July. This can affect the representation of the annual cycle of precipitation in RegCM4.7, as the May–June peak could be underestimated due to unrealistic stronger easterly winds and displacement of the ITCZ to the south of Central America.

Results reported here and elsewhere (Table 1) agree that even for different models and distinct model configurations, underestimation of the CLLJ intensity is usually a common feature. What are the models missing to account for this behavior? Is this characteristic associated with the model representation of the boundary layer in the nested RegCM4.4 model? These questions are addressed in Section 4.

3.2. Precipitation

Mean annual precipitation over the C region from TRMM data (Fig. 6a) is characterized by rates in excess of 8 mm d^{-1} along the ITCZ region and the eastern coasts of Costa Rica and Nicaragua, with a maximum on the west coast of Colombia (>18 mm d^{-1}). In the central Caribbean Sea, rainfall rates are the lowest (<4 mm d^{-1}). A relative minimum in precipitation is also observed off the Pacific coasts of Costa Rica and Nicaragua associated with the CRD, a region of relatively cooler ocean waters. The RegCM4.4 simulations using the G convective scheme, regardless of the domain configuration, adequately reproduce the spatial distribution of annual rainfall (Fig. 6b–e). Note that the model simulations overestimate the mean annual rainfall rate over land areas of Central America, especially in mountain regions, and in the ETP between 4 and 16° N. On the other hand, precipitation is underestimated along the Pacific slope of Colombia and in the westernmost Caribbean Sea. In the former region, the reason for this behavior is possibly related to both the convection schemes used and weaker cross-equatorial flow in the model simulations.

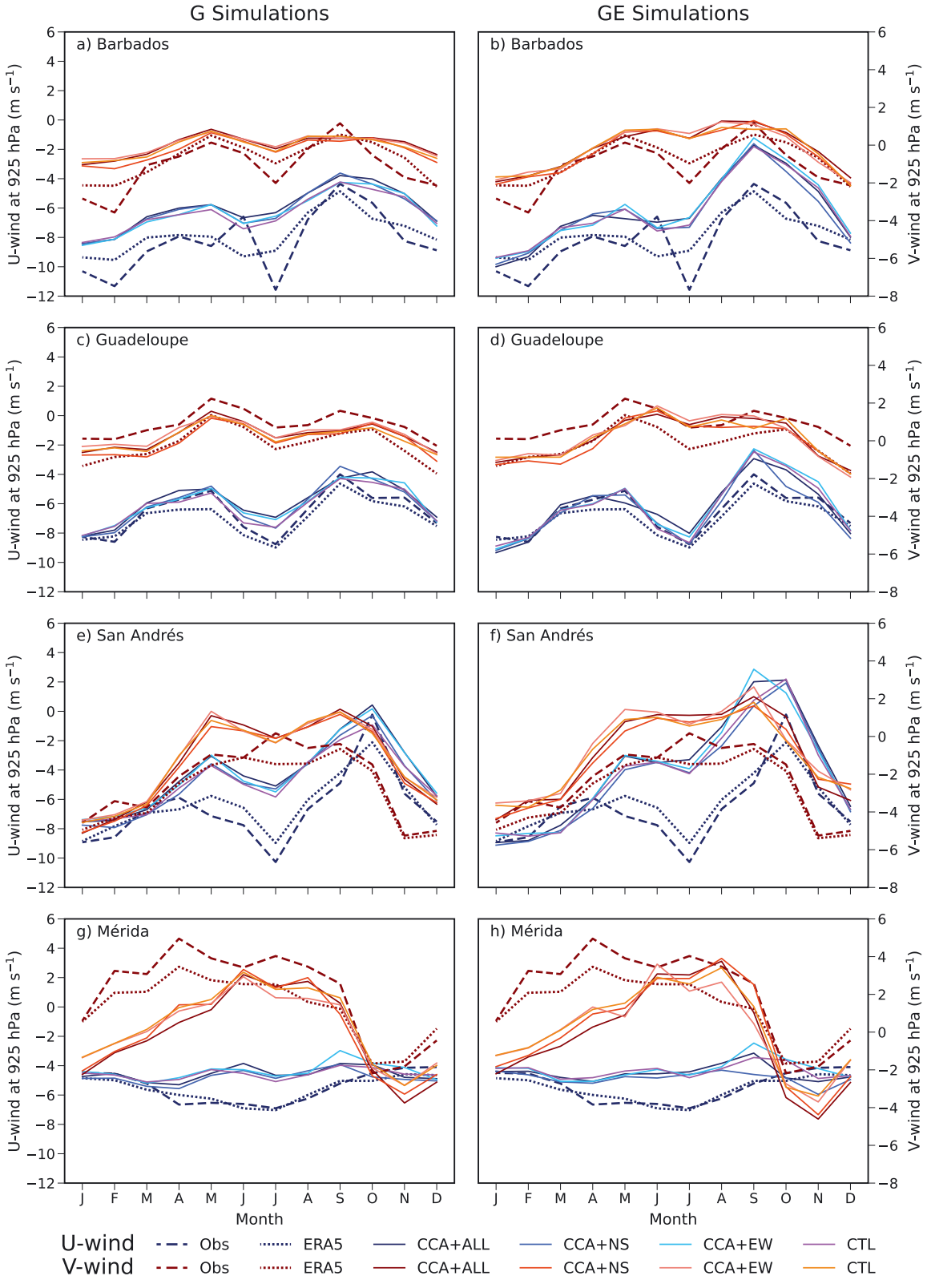

Fig. 4. Observed, ERA5, and modeled mean annual cycle of 925 hPa zonal (U) and meridional (V) wind components during 2006–2011 for (a,b) Grantley Adams, Barbados, (c,d) Le Raizet, Guadeloupe, (e,f) San Andrés, Colombia, and (g,h) Mérida, Mexico. Left (right) panels correspond to RegCM4.4 simulations using G (GE) cumulus parameterization. See Sections 1 and 2 for abbreviations and acronyms

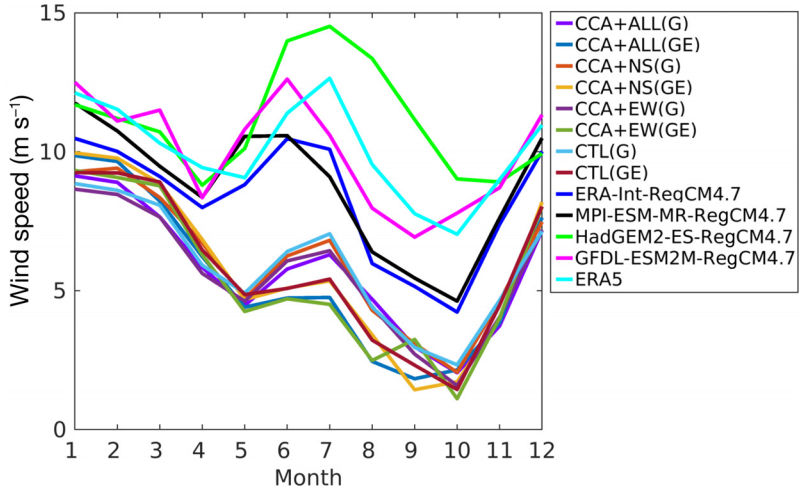

Fig. 5. Annual cycle (2006–2011) of the area-averaged wind speed at 925 hPa over the CLLJ index region for the 8 RegCM4.4 runs used in this work, the RegCM4.7 simulations as described by Torres-Alavez et al. (2021) and ERA5. RegCM4.7 runs forced by the MPI-ESM with mixed resolution (MPI-ESM-MR), the Hadley Centre Global Environment Model-Earth System (HadGEM-ES) and the Geophysical Fluid Dynamics Laboratory Earth System Model version 2M (GFDL-ESM2M) correspond to Representative Concentration Pathways (RCP) 2.6 experiments. See Sections 1 and 2 for abbreviations and acronyms

In February, dry conditions dominate over the western slope of Central America, with rainfall rates <2 mm d^{-1} (Fig. 6f). Along the Caribbean side of the region, there is a relative maximum of precipitation associated with enhanced moisture transport due to the intrusion of cold air masses from the northern part of the continent (Sáenz & Amador 2016) and the intensification of the CLLJ. The ITCZ reaches its southernmost position during this time of year. These features are realistically represented by the G simulations (Fig. 6g–j), although the ITCZ in the model runs is displaced to the north compared with TRMM. In addition, the RegCM4.4 model produces more precipitation in the ITCZ region and the Central America isthmus. The Pacific coast of Colombia is consistently drier in all experiments. The G simulations show a notable overestimation of the precipitation rate over the Caribbean side of both Costa Rica and Nicaragua, an issue probably related to the convection scheme response to the low-level convergence in the CLLJ exit region (Amador 2008, Hidalgo et al. 2015).

During July, TRMM shows the ITCZ located between 6 and 8° N in the ETP and maximum rainfall rate in the southwestern Caribbean Sea (Fig. 6k). Precipitation rates are lower in the Pacific coast of Central America than in the Caribbean coast, and they correspond to the MSD conditions. The G experiments appropriately capture the observed spatial distribution of rainfall (Fig. 6l–o), although rates on the eastern coasts of Costa Rica and Nicaragua are smaller than observed. These differences in precipitation rate between the G simulations and TRMM can also be seen in Fig. S3.

Comparisons between the precipitation rates from the G and GE simulations are shown in Fig. 7. The annual rainfall rates in the G experiments are much smaller on the Pacific side of Central America than in GE (Fig. 7a–d), with absolute differences of 4 mm d^{-1} or more. The opposite occurs on the Caribbean side of Costa Rica and Nicaragua. In February (Fig. 7e–h), the southeastern part of Central America is rainier in the G simulations than in GE. During July (Fig. 7i–l), the simulations with the GE configuration present unrealistically large precipitation rates along the Pacific coast of Central America and lower rates along the Caribbean coast compared with those of G. The much weaker summertime CLLJ in the RegCM4.4 simulations, regardless of cumulus parametrizations used, leads to an anomalous northward displacement of the ITCZ, which is in agreement with the conceptual model proposed by Hidalgo et al. (2015). This results in greater precipitation on the Pacific coast of Central America and reduced rainfall on the Caribbean side due to a weaker CLLJ and less moisture flux convergence over the western Caribbean Sea.

Over the entire subdomain C, Table 2 shows that the annual mean precipitation rate bias in the GE simulations is almost twice as large as the value in G (1.5 and 0.8 mm d^{-1}, respectively). In February, both sets of experiments perform similarly and exaggerate the precipitation rate. An overall undervalue of the rainfall rate is present in the G experiments during July (bias of −0.6 mm d^{-1}), while GE exhibits overestimation (bias of 0.8 mm d^{-1}). These results indicate that a mixed convection scheme (Grell over land–Emanuel over ocean) has more limitations in representing the magnitude of the precipitation in Central America, the western Caribbean Sea, and the ETP.

Fig. 8 shows the mean annual cycle of precipitation over land areas located on the Pacific and Caribbean sides of Central America, using data from CHIRPS, TRMM, and the RegCM4.4 simulations. In the Pacific region (Fig. 8a), there is a rainy season from April–November, with 2 peaks in June and September–October and a reduction in July–August associated with the MSD. Both G and GE experiments produce

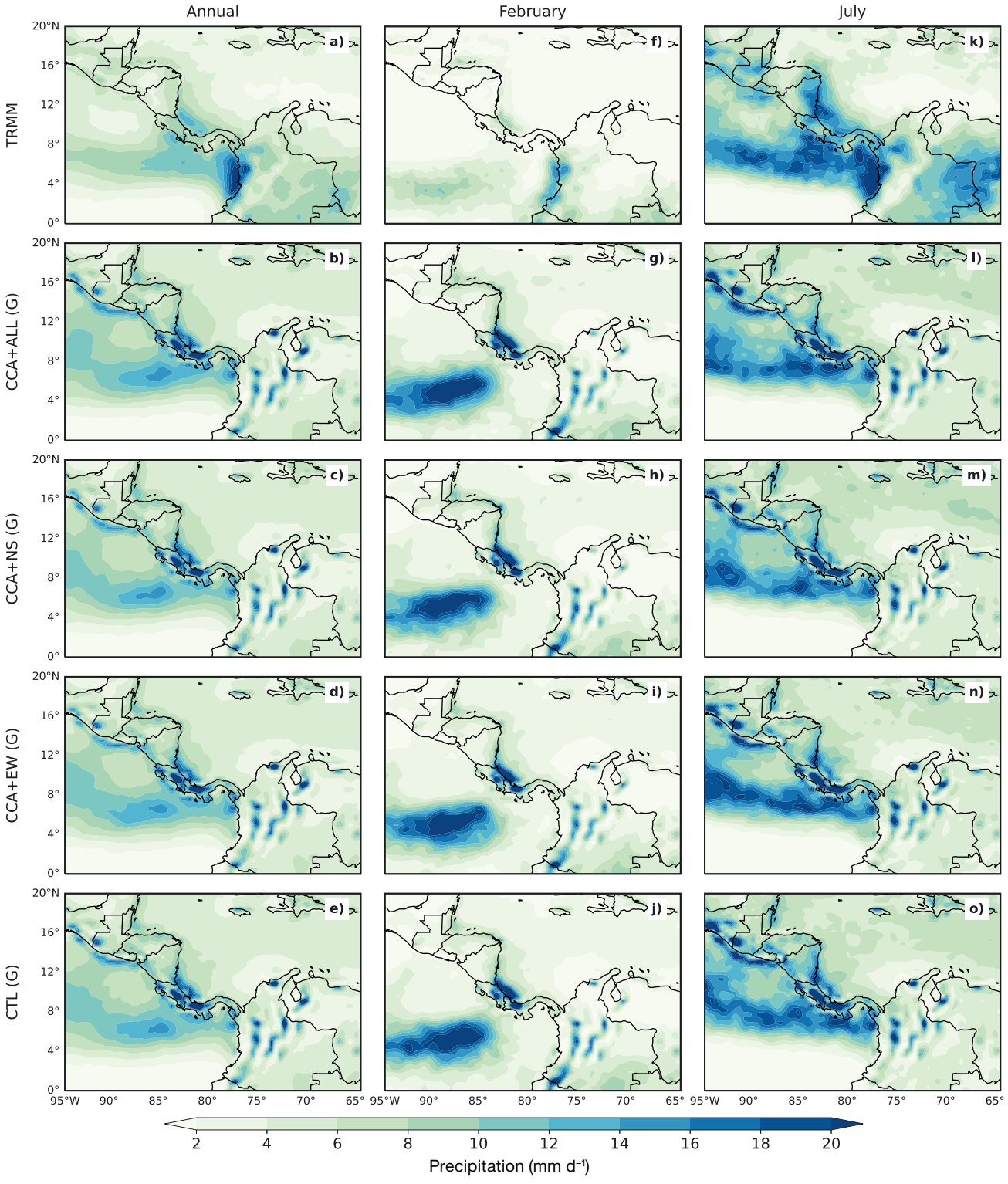

Fig. 6. Same as Fig. 2, but for precipitation rate

very large rainfall rates and do not strictly follow the observed annual cycle of precipitation. In the former, the first maximum occurs in May and the MSD takes place in June–July, which is earlier than observed. In the latter, the first precipitation peak coincides with that of CHIRPS and TRMM, but the MSD is either shorter in duration (only found in July) or not present at all, as in the case of the GE run for CCA+ALL.

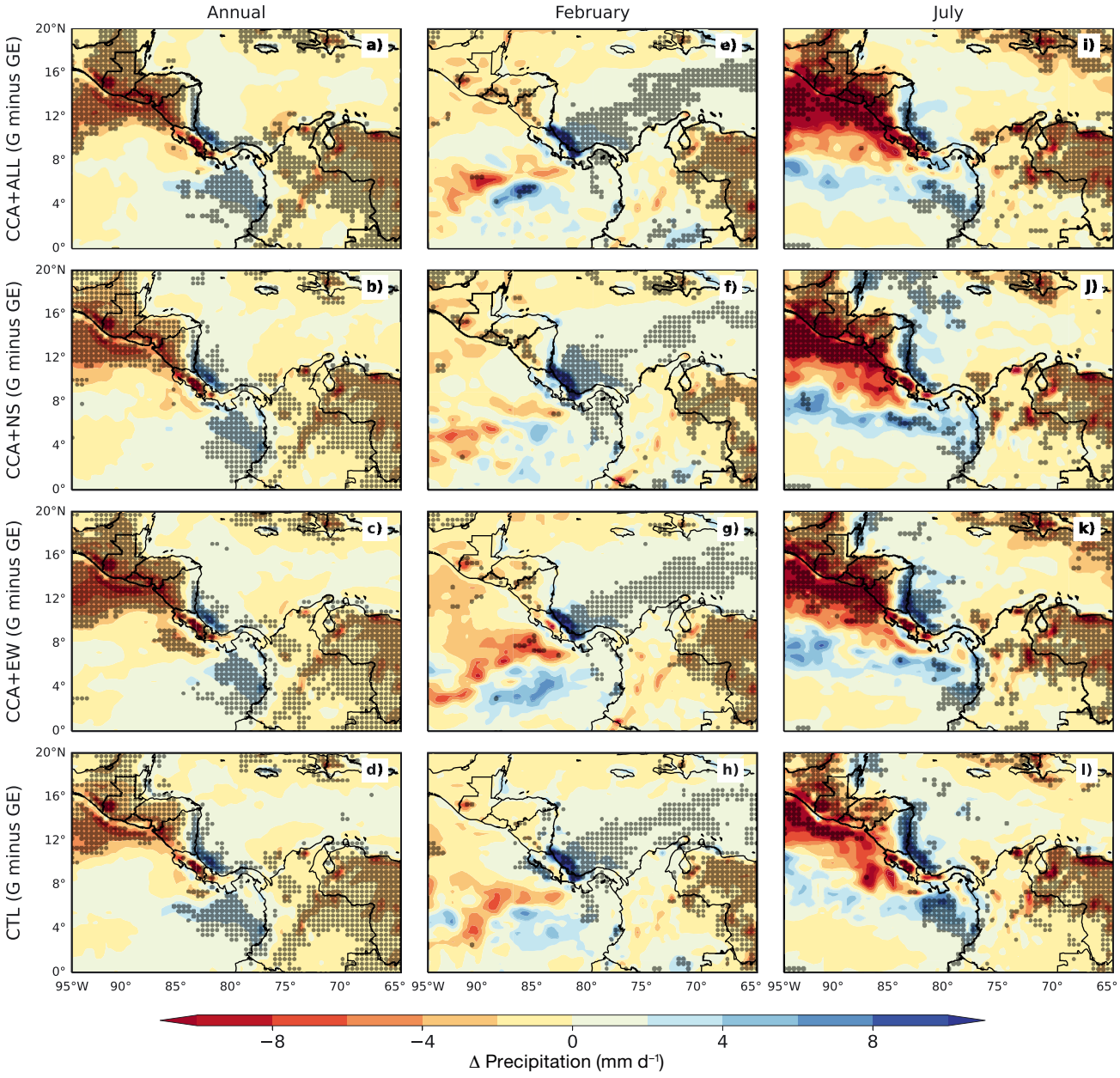

Fig. 7. Same as Fig. 3, but for precipitation rate

On the Caribbean side of Central America (Fig. 8b), both CHIRPS and TRMM show a rainfall distribution with maxima in October–January and June–August and 2 minima in February–April and September. The G and GE simulations fail to appropriately represent the annual cycle of precipitation in this region, which is related to the aforementioned limitations in representing the winter and summer intensities of the CLLJ.

The annual and seasonal precipitation distribution as well as biases in the model results are heavily determined by the cumulus scheme used, while domain size has less impact on the differences between reference precipitation fields and RegCM4.4 simulations.

3.3. Taylor diagrams

Fig. 9 presents Taylor diagrams to compare, over subdomain C, the simulated low-level wind and precipitation with reference fields (ERA5 and TRMM, respectively). Fig. 9a shows that the representation of the zonal wind for February in both sets of simulations — G (red markers) and GE (blue markers) — is

Table 2. Mean precipitation rate bias over subdomain C (0–20° N, 65–95° W). See Section 2 for abbreviations and acronyms

Convection scheme	Domain	Mean precipitation rate bias (mm d^{-1}) Annual	February	July
G	CCA+ALL	0.8	2.5	−0.7
	CCA+NS	0.7	2.4	−0.6
	CCA+EW	0.8	2.4	−0.6
	CTL	0.7	2.4	−0.5
	Overall mean	**0.8**	**2.4**	**−0.6**
GE	CCA+ALL	1.6	2.7	1.3
	CCA+NS	1.5	2.4	0.6
	CCA+EW	1.7	2.7	0.7
	CTL	1.3	2.4	0.5
	Overall mean	**1.5**	**2.5**	**0.8**

very similar in terms of spatial correlation and RMSE. However, the spatial variability in the experiments using the mixed convection scheme is closer to that of ERA5. For the same variable but in July, the G experiments performed better than those using GE, as seen in Fig. 9b.

For meridional wind during February (Fig. 9c), all simulations have similar performance metrics, but GE experiments represent spatial variability better. In the case of July (Fig. 9d), model runs under the G cumulus scheme have higher pattern correlations and their standard deviations, especially in CTL, coincide more with the reference field.

Both groups of simulations overestimate the spatial variability of precipitation in February, but the G experiments have the best performance in terms of pattern correlations and RMSE (Fig. 9e). During July, the latter showed a much closer spatial variability than that of TRMM, higher correlations, and lower RMSE values (Fig. 9f).

3.4. SPI index

Calculation of the SPI index using CHIRPS and RegCM4.4 grid points on the Pacific and Caribbean sides of Central America allows us to assess the model's ability to capture dry and wet periods at different temporal scales, ranging from relatively short modes (3–6 mo) to longer modes (24 mo).

Fig. 10a presents the SPI from monthly CHIRPS data for the Pacific side. From late 2007 to early 2009, the region was characterized by a period of enhanced precipitation at several timescales (SPI-1 to SPI-24), followed by drier conditions from mid-2009 to early 2010. Afterward, there is an alternation between wet and dry periods as shown in SPI-1 to SPI-12. The RegCM4.4 G simulations (Fig. 10b–e) properly capture the observed SPI values. Table 3 shows that the Pearson correlations between CHIRPS and RegCM4.4 (G and GE simulations) SPI time series are relatively high (above 0.4), particularly for SPI-18 and SPI-24, and statistically significant at the 95% BCa confidence level. Despite the wet biases on the Pacific side of Central America, as described previously, the RegCM4.4 shows some

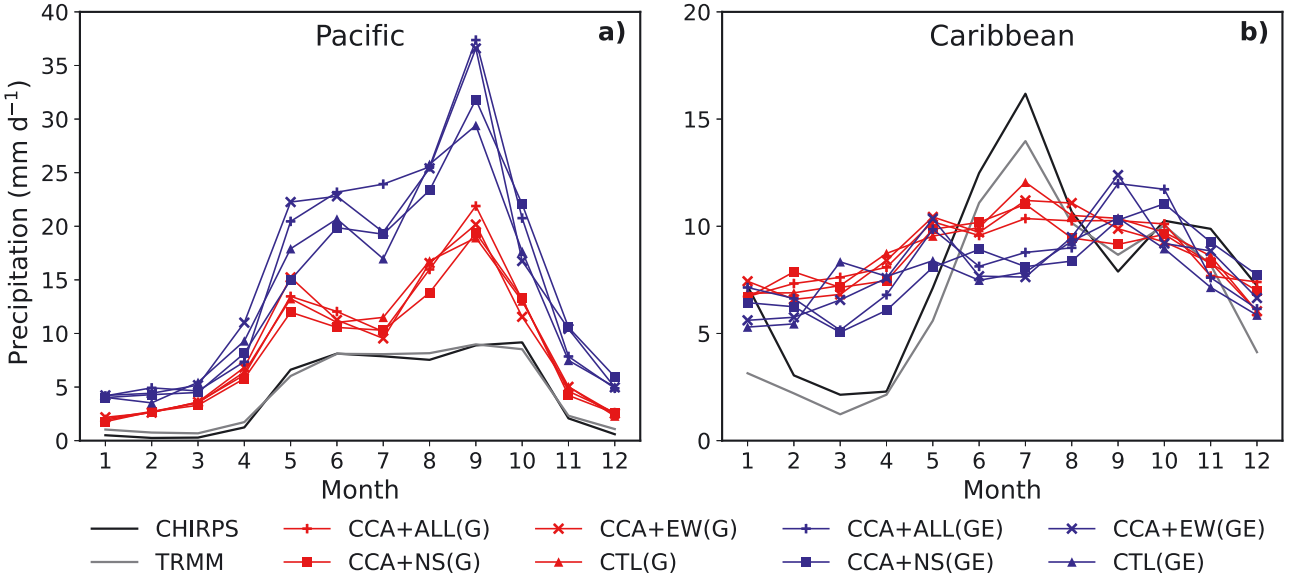

Fig. 8. Annual cycle (2006–2011) of precipitation for the (a) Pacific and (b) Caribbean sides of Central America (as defined in Fig. 1b), using data from CHIRPS, TRMM, and the 8 RegCM4.4 simulations. See Sections 1 and 2 for abbreviations and acronyms

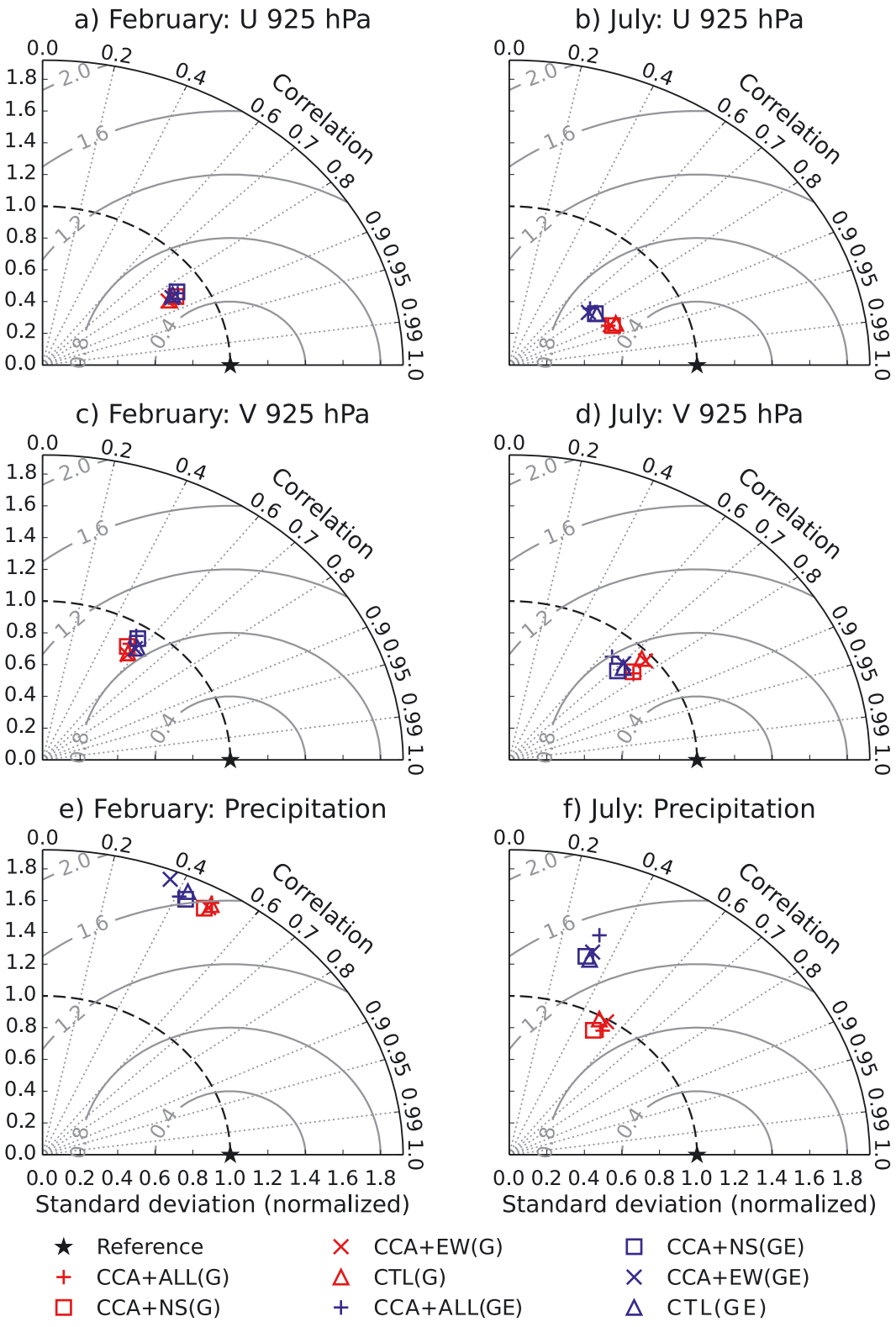

Fig. 9. Taylor diagrams depicting spatial correlations, normalized standard deviations, and centered root mean square error for the 8 model simulations of February and July (a) zonal (U) and (b) meridional (V) wind at 925 hPa (units: m s^{-1}) and (e,f) precipitation rate (units: mm d^{-1}) during 2006–2011. Reference wind (precipitation) fields are derived from ERA5 (TRMM) data. The calculations are performed over subdomain C. All correlations are statistically significant at the 95% bias-corrected and accelerated confidence level. See Sections 1 and 2 for abbreviations and acronyms

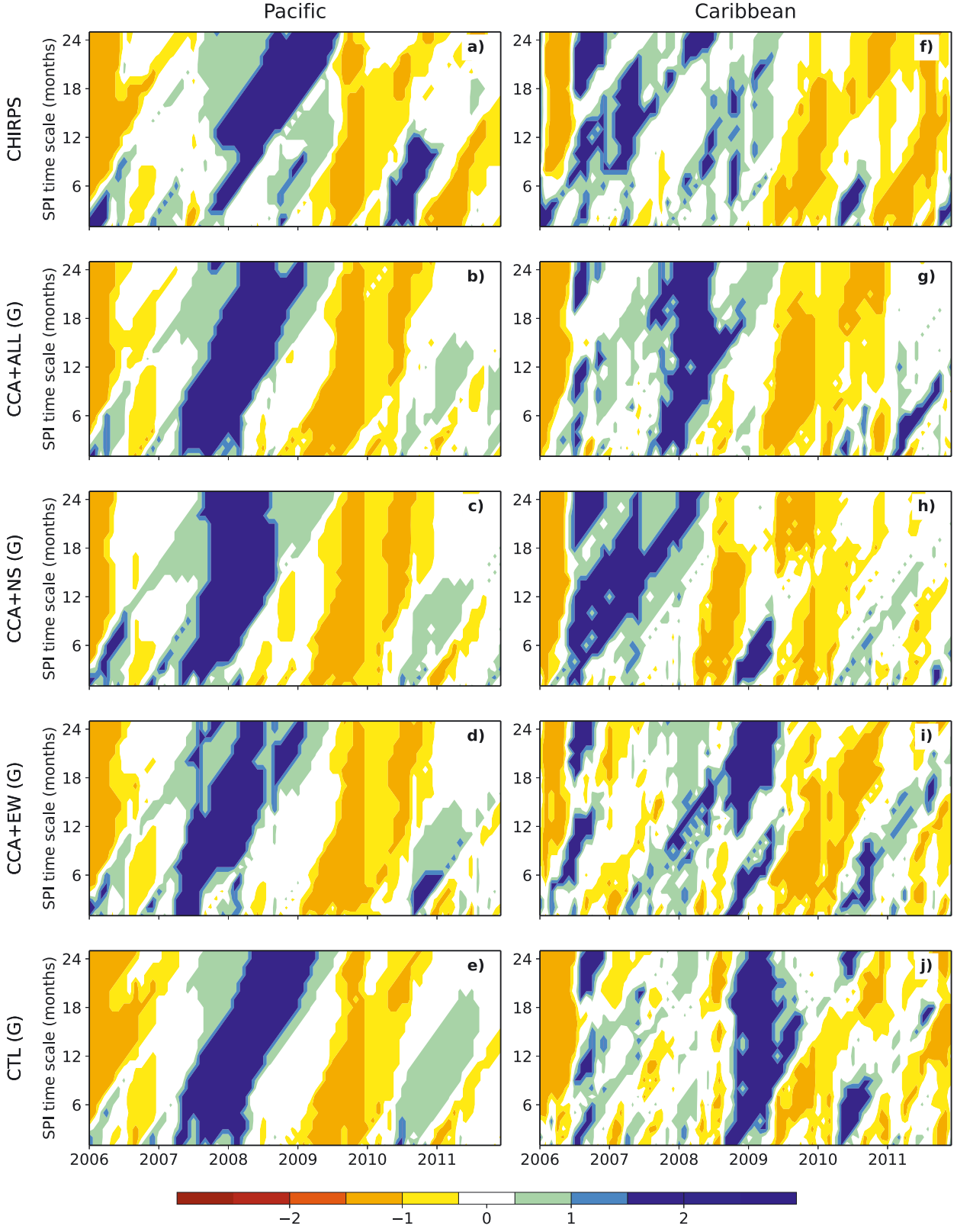

Fig. 10. Standardized precipitation index (1–24 month accumulations) for (a,f) CHIRPS and RegCM4.4 G simulations using the (b,g) CCA+ALL, (c,h) CCA+NS, (d,i) CCA+EW, and (e,j) CTL domain configuration. Left (right) panels correspond to values in the Pacific (Caribbean) side of Central America (as defined in Fig. 1b). See Sections 1 and 2 for abbreviations and acronyms

Table 3. Pearson correlation coefficients between CHIRPS and RegCM4.4 standardized precipitation index (SPI) time series for each of the modeling experiments and for the Pacific and Caribbean regions of Central America. Values in **bold** indicate statistically significant correlations at the 95% bias-corrected and accelerated confidence level. See Sections 1 and 2 for abbreviations and acronyms

SPI time scale (months)	CCA+ALL G	CCA+ALL GE	CCA+NS G	CCA+NS GE	CCA+EW G	CCA+EW GE	CTL G	CTL GE
Pacific region								
6	**0.54**	**0.61**	**0.60**	**0.67**	**0.44**	**0.41**	**0.64**	**0.54**
12	**0.69**	**0.78**	**0.63**	**0.75**	**0.62**	**0.63**	**0.77**	**0.59**
18	**0.85**	**0.91**	**0.76**	**0.91**	**0.83**	**0.88**	**0.90**	**0.73**
24	**0.75**	**0.84**	**0.69**	**0.81**	**0.70**	**0.78**	**0.79**	**0.63**
Caribbean region								
6	**0.24**	**0.43**	**0.42**	**0.50**	**0.46**	−0.07	**0.52**	0.09
12	**0.53**	**0.26**	**0.39**	**0.29**	**0.44**	0.14	**0.51**	0.08
18	**0.55**	**0.40**	**0.43**	**0.40**	**0.45**	**0.41**	0.27	**0.27**
24	**0.78**	**0.42**	**0.59**	**0.65**	**0.61**	**0.51**	**0.47**	**0.50**

ability to represent the temporal variability of precipitation in this region, especially for longer timescales.

In the case of the Caribbean region, Fig. 10f shows the SPI derived from CHIRPS. The period from mid-2006 to early 2009 presented normal to wet conditions at several timescales. Subsequently, the region was drier, except for the wet conditions in mid-2010, as shown in SPI-1 to SPI-6. The modeled SPI values vary substantially depending on the domain configuration (Fig 10g–j). Additionally, the Pearson correlation coefficients between CHIRPS and RegCM4.4 in the Caribbean side of Central America are generally lower than those in the Pacific for 6, 12, 18, and 24 mo SPI time series. Most of them are statistically significant at the 95% BCa confidence level (Table 3). In general, the G simulations do

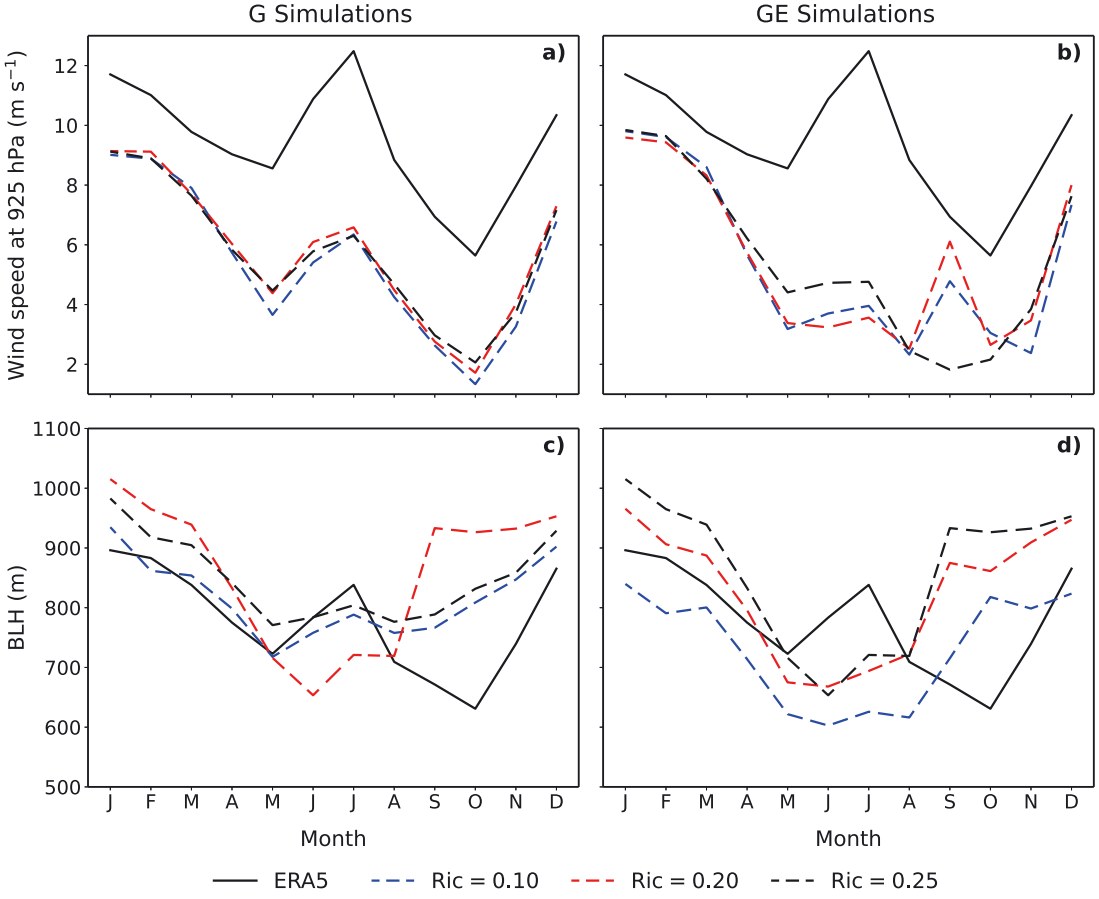

Fig. 11. Mean annual cycle of (a,b) wind at 925 hPa and (c,d) boundary layer height (BLH) during 2006–2011 over the CLLJ index region for ERA5 (black solid line) and RegCM4.4 simulations (CCA+ALL domain), using the critical Richardson number (Ric) equal to 0.25, 0.20, and 0.10. Left (right) panels correspond to simulations using the G (GE) setup. See Sections 1 and 2 for abbreviations and acronyms

not properly represent the pattern of precipitation variability in this region.

3.5. Sensitivity of the CLLJ intensity to the choice of the Ric

The notorious weakening of the simulated summertime CLLJ intensity, as described in Section 3.1, may be due to the boundary layer representation in the Holtslag PBL scheme. In this parameterization, the BLH is dependent on the Ric number (Holtslag et al. 1990). The top panels of Fig. 11 show the mean annual cycle of low-level wind speed in the CLLJ index region from ERA5 and RegCM4.4 (CCA+ALL domain), using 3 different values of Ric: 0.25, 0.20, and 0.10. ERA5 wind intensity at 925 hPa is considerably larger than simulated. In the RegCM4.4 G experiments, a reduction of Ric from the default value of 0.25 to 0.20 and 0.10 results in practically no changes in the magnitude of wind at the CLLJ region (Fig. 11a). In the case of the GE runs (Fig. 11b), 925 hPa wind speeds from November–April are essentially the same for the 3 Ric values, while reduction (increase) in intensity occurs in May–July (September–October) when using Ric equal to 0.20 and 0.10.

Contrary to expectations, a reduction of Ric in the Holtslag boundary layer scheme does not translate into changes in the CLLJ intensity, although the depth of the BLH over the CLLJ index region experiences some variations. According to ERA5, the BLH has 2 maxima in December–February and July. Both G and GE simulations capture the boreal winter maximum but present difficulties in reproducing the peak in July, particularly the GE experiments, regardless of the selected Ric number (Fig. 11c,d). This misrepresentation of the boreal summer characteristics of the PBL could partially explain the model's deficiencies in simulating the summertime CLLJ strength.

4. DISCUSSION

In this work, the CCA domain at 50 km (0.44°) horizontal resolution with a relaxation zone of 10° around the boundaries was taken as the basis to increase the domain size in the RegCM4.4 model. The sensitivity of the precipitation and atmospheric low-level circulation patterns to domain size changes and the choice of physical parameterizations in this regional model were tested. The RegCM4.4 model simulations were driven by ERA-Interim data starting on 1 January 2005 (at 00:00 h UTC) and run continuously for 7 yr until 1 January 2012 (at 00:00 h UTC). The first year was excluded from the analysis to allow the model to spin-up. Three sets of experiments were analyzed. In the first, the Grell precipitation scheme was used for all runs. The second set used a mixed convection approach (Grell over land–Emanuel over ocean). The last experiment, limited to one domain configuration (CCA+ALL), implemented reductions in the value of Ric over both land and ocean within the Holtslag PBL scheme to assess its effect on the boundary layer characteristics (especially over the Caribbean Sea) and the representation of the CLLJ intensity.

Mean fields estimated from observations and reanalysis data were used to test the ability of the model to capture regional climatic features, such as the CLLJ and MSD. The low-level circulation patterns and precipitation distribution over Central America and southern Mexico do not show strong sensitivity to domain size changes for an area increment of 18, 32, and 52 % with respect to the size of the control domain (CCA+ or CTL). This implies that the current domain configuration as formulated by the CORDEX initiative is suitable for the simulation of regional climate characteristics and atmospheric processes. For Central America, the western Caribbean Sea, and the ETP, changes in the size of the CCA domain has less impact than the choice of cumulus parameterization schemes or changes in physical parameters associated with the PBL representation.

Simulated 925 hPa winds over the Caribbean Sea and the CLLJ region showed some features of the observed seasonal behavior, such as the low-level winter and summer maxima of the zonal component, but in general, the intensity of these peaks was weaker, especially in July (similar results for boreal summer were reported by Martínez-Castro et al. 2018). This has enormous implications for (1) the summertime position of the ITCZ, as the CLLJ has a greater influence on the low-level moisture convergence and precipitation patterns in Central America during this time of year than SST distribution in the ETP (García-Franco et al. 2022), and (2) moisture transport over the Caribbean Sea region, the Gulf of Mexico, and the Great Plains of the USA. Shifts in the expected location of the ITCZ in RegCM4 historical simulations were also reported by Fuentes-Franco et al. (2014).

Although the differences in summer wind magnitude between the G and GE simulations over the Caribbean Sea region are not statistically significant, they have been related by Martínez-Castro et al. (2018) to the influence of deep convection on the CLLJ inten-

sity. Hidalgo et al. (2015) proposed a scheme for the interaction between the CLLJ and the zonal distribution of precipitation. In that framework, vertical motion associated with the strong convective region between Costa Rica and Nicaragua generates eastward wind at the top of the atmosphere and subsidence on the central Caribbean Sea, presumably affecting the intensity of the low-level jet. Li et al. (2018) partially discussed the relationship of convection with the ENSO wind regime in a study over the western equatorial Pacific (WEP), indicating that wind anomalies may be induced by convection anomalies over the WEP during spring. Other works have shown that large-scale circulation biases in regional model simulations may be linked to the cumulus parameterization schemes (for example, Giorgi & Shields 1999 and Diro et al. 2012). The reason is that these parameterizations differ in the way they represent feedback to the large-scale environment, moisture processes, and the triggering of convection (Hu et al. 2020).

The regional model simulations also fail to appropriately represent the sign of the meridional wind during the boreal winter (positive in the Gulf of Mexico and negative in the eastern Caribbean Sea near the CLLJ entrance), which can result in underestimation of the transport of moisture to the Venezuela Grandes Llanos low-level jet in northern South America and its connection with the South America low-level jet (Montini et al. 2019). Such conditions also affect the representation of cold air intrusions into Central America during this time of year, which is an important mechanism for precipitation distribution over the region's Caribbean slope.

The RegCM4.4 model under both G and GE cumulus parameterizations does not fully capture key precipitation patterns, especially regional characteristics such as the MSD and the southwestern Caribbean Sea maxima. However, for precipitation, G experiments perform better than those using the mixed GE setup. These results contrast with previous findings for the CCA domain (Diro et al. 2012) and other CORDEX regions (Giorgi et al. 2012). Martínez-Castro et al. (2018) also found that the mixed convection scheme of GE is not capable of reproducing the MSD signal. In their work, a tuned version of the Tiedtke convection scheme for the CCA domain at a spatial resolution of 25 km showed the smallest errors.

Modeled dry and wet spells based on SPI appear to respond better for longer timescales (18 and 24 months), especially in the Pacific slope of Central America, which is possibly related to the control by boundary conditions like SST. Most of the correlations between SPI time series from CHIRPS and those from RegCM4.4 are statistically significant for timescales shorter than or equal to 24 mo. Although RegCM4.4 simulations fail to correctly represent the observed precipitation rates, the SPI analysis is a useful tool to evaluate the ability of the regional model to capture the temporal variability of precipitation at several timescales. For example, Bowden et al. (2016) performed an 18 yr regional model simulation on a 36 km grid covering the contiguous USA and used SPI to determine the added value of dynamical downscaling in assessing the timing and severity of wet and dry episodes over different climate regions.

The weakened summer circulations in the Reg CM4.4 model have implications for the precipitation distribution during the rainy season in Central America. Changing the value of Ric in the Holtslag scheme did not induce changes in the representation of the boreal summer CLLJ maximum at 925 hPa. The July PBL depth was underestimated in model simulations over the CCA+ALL domain, regardless of the choice of Ric. Model deficiencies in representing the PBL characteristics could partially be related to the problems in simulating the CLLJ intensity during this time of year. Zhang et al. (2015) performed similar sensitivity experiments using a global climate model and found a linear increase in the simulated global mean of BLH as the value of Ric grows. Nonetheless, the impact of changing Ric on the globally averaged wind speed was weak.

Problems in representing the CLLJ correctly are common in the simulations performed in this work as well as in other studies and experiments for Central America and the Caribbean. Even higher-resolution simulations, such as those of Martínez et al. (2019) and Torres-Alavez et al. (2021), which used 45 and 23 vertical levels, respectively, on 25 km horizontal grids, have shown some deficiencies in reproducing the observed intensity of the CLLJ and the timing of its winter and summer maxima. Questions arise about the missing physical mechanisms in the models to account for this behavior. The representation of the boundary layer in regional models can be crucial for adequately capturing the summer maximum of the CLLJ. In addition, the interactions and feedback among the cumulus parameterizations, the boundary layer schemes, and the large-scale circulation can play an important role in determining the simulated CLLJ properties.

Further studies based on multiphysics ensembles of longer-term runs with increased horizontal and vertical resolutions are therefore necessary to understand the influence of the parameterization schemes and the model configurations on climate simulations

over the CCA domain. The future application of a coupled ocean–atmosphere model in the region may also provide a better representation of key climate features, such as the CLLJ and MSD.

Acknowledgements. This research was funded by the University of Costa Rica (Grants VI-805-A4-906/A5-719/B0-810/B5-296/B8-604//B9-454/B9-609). The Center for Geophysical Research (CIGEFI), University of Costa Rica, provided computational facilities (Tsaheva cluster) to perform the numerical simulations presented in this study (more than 1000 h of computing time were required). We acknowledge the World Climate Research Program's Working Group on Regional Climate and the Working Group on Coupled Modeling, former coordinating body of CORDEX and responsible panel for CMIP5. We also thank the ICTP climate modeling group, especially José Abraham Torres-Alavez, for producing and making available their model output. We also acknowledge the Earth System Grid Federation infrastructure, an international effort led by the US Department of Energy's Program for Climate Model Diagnosis and Intercomparison, the European Network for Earth System Modeling, and other partners in the Global Organization for Earth System Science Portals (GO-ESSP). SPI values were calculated with the routine developed by Joseph Wheatley and Ángel G. Muñoz. The code by Yannick Copin (https://gist.github.com/ycopin/3342888) was used for plotting the Taylor diagrams. Lastly, we thank Natali Mora, Carlos Madrigal, Felipe González, and Daniel Chacón for providing support during this work and the 4 anonymous reviewers for their comments on the manuscript.

LITERATURE CITED

Amador JA (1998) A climatic feature of the tropical Americas: the trade wind easterly jet. Top Meteorol Oceanogr 5:91–102

Amador JA (2008) The intra-Americas seas low-level jet (IALLJ): overview and future research. Ann NY Acad Sci 1146:153–188

Amador JA (2011) Socioeconomic impacts associated with meteorological systems and tropical cyclones in Central America in 2010. Bull Am Meteorol Soc 92:S184–S189

Amador JA, Alfaro EJ (2009) Métodos de reducción de escala: aplicaciones al tiempo, clima, variabilidad climática y cambio climático. Rev Iberoam Econ Ecol 11:39–52

Amador JA, Alfaro EJ (2014) Weather and climate socioeconomic impacts in Central America for the management and protection of world heritage sites and the Diquis Delta culture in Costa Rica (a case study). Adv Geosci 35:157–167

Amador JA, Arce-Fernández D (2022) WWLLN hot and cold-spots of lightning activity and their relation to climate in an extended Central America region 2012–2020. Atmosphere (Basel) 13:76

Amador JA, Rivera ER, Durán-Quesada AM, Mora G, Sáenz F, Calderón B, Mora N (2016a) The easternmost tropical Pacific. I. A climate review. Rev Biol Trop 64:1–22

Amador JA, Durán-Quesada AM, Rivera ER, Mora G, Sáenz F, Calderón B, Mora N (2016b) The easternmost tropical Pacific. II. Seasonal and intraseasonal modes of atmospheric variability. Rev Biol Trop 64:23–57

Arakawa A, Schubert WH (1974) Interaction of a cumulus cloud ensemble with the large-scale environment. I. J Atmos Sci 31:674–701

Arce-Fernández D, Amador JA (2021) Actividad eléctrica asociada al huracán Otto (2016) en el Mar Caribe y en el Corredor Seco Centroamericano. Rev Bras Meteorol 36: 1–13

Artale V, Calmanti S, Carillo A, Dell'Aquila A and others (2010) An atmosphere–ocean regional climate model for the Mediterranean area: assessment of a present climate simulation. Clim Dyn 35:721–740

Beck HE, Westra S, Tan J, Pappenberger F and others (2020) PPDIST, global 0.1° daily and 3-hourly precipitation probability distribution climatologies for 1979–2018. Sci Data 7:302

Bhaskaran B, Ramachandran A, Jones R, Moufouma-Okia W (2012) Regional climate model applications on sub-regional scales over the Indian monsoon region: the role of domain size on downscaling uncertainty. J Geophys Res 117:D10113

Bowden JH, Talgo KD, Spero TL, Nolte CG (2016) Assessing the added value of dynamical downscaling using the standardized precipitation index. Adv Meteorol 2016: 8432064

Cabos W, Sein DV, Durán-Quesada A, Liguori G and others (2019) Dynamical downscaling of historical climate over CORDEX Central America domain with a regionally coupled atmosphere–ocean model. Clim Dyn 52:4305–4328

Centella-Artola A, Taylor MA, Bezanilla-Morlot A, Martínez-Castro D, Campbell JD, Stephenson TS, Vichot A (2015) Assessing the effect of domain size over the Caribbean region using the PRECIS regional climate model. Clim Dyn 44:1901–1918

Centella-Artola A, Bezanilla-Morlot A, Taylor MA, Herrera DA and others (2020) Evaluation of sixteen gridded precipitation datasets over the Caribbean region using gauge observations. Atmosphere (Basel) 11:1334

Cook KH, Vizy EK (2010) Hydrodynamics of the Caribbean low-level jet and its relationship to precipitation. J Clim 23:1477–1494

Dee DP, Uppala SM, Simmons AJ, Berrisford P and others (2011) The ERA-Interim reanalysis: configuration and performance of the data assimilation system. QJR Meteorol Soc 137:553–597

DelSole T, Tippett M (2022) Statistical methods for climate scientists. Cambridge University Press, Cambridge

Dickinson R, Henderson-Sellers A, Kennedy PJ (1993) Biosphere–Atmosphere Transfer Scheme (BATS) version 1E as coupled to the NCAR Community Climate Model. NCAR technical note NCAR/TN-3871 STR. National Center for Atmospheric Research, Boulder, CO

Diffenbaugh NS, Giorgi F (2012) Climate change hotspots in the CMIP5 global climate model ensemble. Clim Change 114:813–822

Diro GT, Rauscher SA, Giorgi F, Tompkins AM (2012) Sensitivity of seasonal climate and diurnal precipitation over Central America to land and sea surface schemes in RegCM4. Clim Res 52:31–48

Durán-Quesada AM, Gimeno L, Amador JA, Nieto R (2010) Moisture sources for Central America: identification of moisture sources using a Lagrangian analysis technique. J Geophys Res 115:D05103

Durán-Quesada AM, Gimeno L, Amador JA (2017) Role of moisture transport for Central American precipitation. Earth Syst Dyn 8:147–161

Emanuel KA (1991) A scheme for representing cumulus convection in large-scale models. J Atmos Sci 48:2313–2335
Feng Z, Leung LR, Liu N, Wang J and others (2021) A global high-resolution mesoscale convective system database using satellite-derived cloud tops, surface precipitation, and tracking. J Geophys Res 126:e2020JD034202
Fuentes-Franco R, Coppola E, Giorgi F, Graef F, Pavia EG (2014) Assessment of RegCM4 simulated inter-annual variability and daily-scale statistics of temperature and precipitation over Mexico. Clim Dyn 42:629–647
Funk C, Peterson P, Landsfeld M, Pedreros D and others (2015) The climate hazards infrared precipitation with stations — a new environmental record for monitoring extremes. Sci Data 2:150066
García-Franco JL, Gray LJ, Osprey S (2020) The American monsoon system in HadGEM3 and UKESM1. Weather Clim Dyn 1:349–371
García-Franco JL, Chadwick R, Gray LJ, Osprey S, Adams DK (2022) Revisiting mechanisms of the Mesoamerican midsummer drought. Clim Dyn, doi:10.1007/s00382-022-06338-6
Gimeno L, Dominguez F, Nieto R, Trigo R and others (2016) Major mechanisms of atmospheric moisture transport and their role in extreme precipitation events. Annu Rev Environ Resour 41:117–141
Giorgi F (2006) Climate change hot-spots. Geophys Res Lett 33:L08707
Giorgi F, Shields C (1999) Tests of precipitation parameterizations available in latest version of NCAR regional climate model (RegCM) over continental United States. J Geophys Res 104:6353–6375
Giorgi F, Coppola E, Solmon F, Mariotti L and others (2012) RegCM4: model description and preliminary tests over multiple CORDEX domains. Clim Res 52:7–29
Giorgi F, Elguindi N, Cozzini S, Giuliani G (2014) Regional climatic model RegCM user's guide version 4.4. International Centre for Theoretical Physics, Trieste. http://154.66.220.45:3000/doc/_downloads/RegCM-UserGuide.pdf
Gray WM (1979) Hurricanes: their formation, structure and likely role in the tropical circulation. In: Shaw DB (ed) Meteorology over the tropical oceans. Royal Meteorological Society, Reading, p 155–218
Gray WM, Landsea CW, Mielke PW, Berry KJ (1992) Predicting Atlantic seasonal hurricane activity 6–11 months in advance. Weather Forecast 7:440–455
Gregory D, Rowntree PR (1990) A mass flux convection scheme with representation of cloud ensemble characteristics and stability-dependent closure. Mon Weather Rev 118:1483–1506
Grell G (1993) Prognostic evaluation of assumptions used by cumulus parameterizations. Mon Weather Rev 121:764–787
Hastenrath S (1967) Rainfall distribution and regime in Central America. Arch Meteorol, Geophys Bioklimatol, Ser B Allg Biol Klimatol 15:201–241
Hayes SP, McPhaden MJ, Wallace JM (1989) The influence of sea surface temperature on surface wind in the eastern equatorial Pacific: weekly to monthly variability. J Clim 2:1500–1506
Hersbach H, Bell B, Berrisford P, Hirahara S and others (2020) The ERA5 global reanalysis. QJR Meteorol Soc 146:1999–2049
Hidalgo HG, Alfaro EJ (2015) Skill of CMIP5 climate models in reproducing 20th century basic climate features in Central America. Int J Climatol 35:3397–3421
Hidalgo HG, Durán-Quesada AM, Amador JA, Alfaro EJ (2015) A proposed dynamical mechanism linking Pacific and Caribbean climate. Geogr Ann, Ser A 97:41–59
Holtslag AA, De Bruijn EI, Pan H (1990) A high resolution air mass transformation model for short-range weather forecasting. Mon Weather Rev 118:1561–1575
Hu Y, Zhong Z, Ha Y, Sun Y, Zhu Y, Yu L (2020) Impacts of cumulus parameterization schemes on the simulation of interannual and interdecadal variation of Meiyu in the middle and lower reaches of the Yangtze River by using Regional Climate Model 4. Front Earth Sci 8:588038
Huffman GJ, Adler RF, Bolvin DT, Gu G and others (2007) The TRMM multisatellite precipitation analysis (TMPA): quasi-global, multiyear, combined-sensor precipitation estimates at fine scales. J Hydrometeorol 8:38–55
Kalnay E, Kanamitsu M, Kistler R, Collins W and others (1996) The NCEP/NCAR 40-year reanalysis project. Bull Am Meteorol Soc 77:437–472
Karmalkar AV, Bradley RS, Diaz HF (2011) Climate change in Central America and Mexico: regional climate model validation and climate change projections. Clim Dyn 37:605–629
Kessler WS (2006) The circulation of the eastern tropical Pacific: a review. Prog Oceanogr 69:181–217
Kiehl JT, Hack JJ, Bonan GB, Boville BA and others (1996) Description of the NCAR Community Climate Model (CCM3). NCAR Technical Note NCAR/TN-420+STR. National Center for Atmospheric Research, Boulder, CO
Kouassi A, Kone B, Silue S, Dajuma A and others (2022) Sensitivity study of the RegCM4's surface schemes in the simulations of West Africa climate. Atmos Clim Sci 12:86–104
Landsea CW (1993) A climatology of intense (or major) Atlantic hurricanes. Mon Weather Rev 121:1703–1713
Landsea CW (2005) Hurricanes and global warming. Nature 438:E11–E12
Lara-Estrada L, Rasche L, Schneider UA (2021) Land in Central America will become less suitable for coffee cultivation under climate change. Reg Environ Change 21:88
Leduc M, Laprise R (2009) Regional climate model sensitivity to domain size. Clim Dyn 32:833–854
Li Z, Yang S, Hu X, Dong W, He B (2018) Charge in long-lasting El Niño events by convection-induced wind anomalies over the Western Pacific in boreal spring. J Clim 31:3755–3763
Magaña V, Amador JA, Medina S (1999) The mid-summer drought over Mexico and Central America. J Clim 12:1577–1588
Martínez JA, Arias PA, Castro C, Chang HI, Ochoa-Moya CA (2019) Sea surface temperature-related response of precipitation in northern South America according to a WRF multi-decadal simulation. Int J Climatol 39:2136–2155
Martínez-Castro D, da Rocha RP, Bezanilla-Morlot A, Alvarez-Escudero L and others (2006) Sensitivity studies of the RegCM3 simulation of summer precipitation, temperature and local wind field in the Caribbean region. Theor Appl Climatol 86:5–22
Martínez-Castro D, Vichot-Llano A, Bezanilla-Morlot A, Centella-Artola A and others (2018) The performance of RegCM4 over the Central America and Caribbean region using different cumulus parameterizations. Clim Dyn 50:4103–4126
McKee TB, Doesken NJ, Kleist J (1993) The relationship of drought frequency and duration to time scales. In: Proc 8th Conf on Applied Climatology, 17–22 January 1993,

Anaheim, CA. American Meteorological Society, Boston, MA, p 179–184
Misra V, Jayasankar CB (2022) A high resolution coupled ocean–atmosphere simulation of the regional climate over Central America. Clim Dyn 58:2981–3001
Mo KC, Chelliah M, Carrera ML, Higgins RW, Ebisuzaki W (2005) Atmospheric moisture transport over the United States and Mexico as evaluated in the NCEP regional reanalysis. J Hydrometeorol 6:710–728
Montini TL, Jones C, Carvalho LMV (2019) The South American low-level jet: a new climatology, variability, and changes. J Geophys Res 124:1200–1218
Mora N, Amador JA, Rivera ER, Maldonado T (2020) A sea breeze study during Ticosonde-NAME 2004 in the Central Pacific of Costa Rica: observations and numerical modeling. Atmosphere (Basel) 11:1333
Moron V, Robertson AW (2021) Relationships between subseasonal-to-seasonal predictability and spatial scales in tropical rainfall. Int J Climatol 41:5596–5624
Ortega G, Arias PA, Villegas JC, Marquet PA, Nobre P (2021) Present-day and future climate over Central and South America according to CMIP5/CMIP6 models. Int J Climatol 41:6713–6735
Pal JS, Small EE, Eltahir EAB (2000) Simulation of regional-scale water and energy budgets: representation of subgrid cloud and precipitation processes within RegCM. J Geophys Res 105:29579–29594
Pant M, Ghosh S, Verma S, Sinha P and others (2022) Simulation of an extreme rainfall event over Mumbai using a regional climate model: a case study. Meteorol Atmos Phys 134:9
Pareja-Quispe D, Franchito SH, Fernandez JPR (2021) Assessment of the RegCM4 performance in simulating the surface radiation budget and hydrologic balance variables in South America. Earth Syst Environ 5:499–518
Patz JA, Kovats RS (2002) Hotspots in climate change and human health. BMJ 325:1094–1098
Rivera ER, Amador JA (2008) Predicción estacional del clima en Centroamérica mediante la reducción de escala dinámica. I. Evaluación de los modelos de circulación general CCM3.6 y ECHAM4.5. Rev Mat Teoria Apl 15:131–173
Rivera ER, Amador JA (2009) Predicción estacional del clima en Centroamérica mediante la reducción de escala dinámica. II. Aplicación del modelo MM5v3. Rev Mat Teoria Apl 16:76–104
Sáenz F, Amador JA (2016) Características del ciclo diurno de precipitación en el Caribe de Costa Rica. Rev Climatol 16:21–34
Serra YL, Jiang X, Tian B, Amador JA, Maloney ED, Kiladis GN (2014) Tropical intraseasonal oscillations and synoptic variability. Annu Rev Environ Resour 39:189–215
Seth A, Giorgi F (1998) The effects of domain choice on summer precipitation simulation and sensitivity in a regional climate model. J Clim 11:2698–2712
Stewart IT, Maurer EP, Stahl K, Joseph K (2022) Recent evidence for warmer and drier growing seasons in climate sensitive regions of Central America from multiple global datasets. Int J Climatol 42:1399–1417
Stickler A, Grant AN, Ewen T, Ross TF and others (2010) The comprehensive historical upper-air network. Bull Am Meteorol Soc 91:741–752
Suga R, Megyeri-Korotaj OA, Allaga-Zsebeházi G (2021) Sensitivity study of the REMO regional climate model to domain size. Adv Sci Res 18:157–167
Takahashi H, Lebsock M, Luo ZJ, Masunaga H, Wang C (2021) Detection and tracking of tropical convective storms based on globally gridded precipitation measurements: algorithm and survey over the tropics. J Appl Meteorol Climatol 60:403–421
Taylor KE (2001) Summarizing multiple aspects of model performance in a single diagram. J Geophys Res 106: 7183–7192
Taylor MA, Whyte FS, Stephenson TS, Campbell JD (2013) Why dry? Investigating the future evolution of the Caribbean Low Level Jet to explain projected Caribbean drying. Int J Climatol 33:784–792
Torres-Alavez JA, Das S, Corrales-Suastegui A, Coppola E and others (2021) Future projections in the climatology of global low-level jets from CORDEX-CORE simulations. Clim Dyn 57:1551–1569
Vannitsem S, Chomé F (2005) One-way nested regional climate simulations and domain size. J Clim 18:229–233
Velasco I, Fritsch JM (1987) Mesoscale convective complexes in the Americas. J Geophys Res 92:9591–9613
Vichot-Llano A, Martínez-Castro D, Centella-Artola A, Bezanilla-Morlot A (2014) Sensibilidad al cambio de dominio y resolución de tres configuraciones del modelo climático regional RegCM 4.3 para la región de América Central y el Caribe. Rev Climatol 14:45–62
Vichot-Llano A, Martínez-Castro D, Bezanilla-Morlot A, Centella-Artola A and others (2022) Caribbean low-level jet future projections using a multiparameter ensemble of RegCM4 configurations. Int J Climatol 42: 1544–1559
Villafuerte MQ, Lambrento JCR, Hodges KI, Cruz FT and others (2021) Sensitivity of tropical cyclones to convective parameterization schemes in RegCM4. Clim Dyn 56: 1625–1642
Wang C, Enfield DB (2001) The tropical Western Hemisphere warm pool. Geophys Res Lett 28:1635–1638
Wang C, Enfield DB (2003) A further study of the tropical Western Hemisphere warm pool. J Clim 16:1476–1493
WMO (2012) Standardized precipitation index user guide. WMO-No. 1090. World Meteorological Organization, Geneva
Yu C, Li Z, Blewitt G (2021) Global comparisons of ERA5 and the operational HRES tropospheric delay and water vapor products with GPS and MODIS. Earth Space Sci 8: e2020EA001417
Yu Z, Wu M, Min J, Yan Y, Lou X (2022) Impacts of WRF model domain size on Meiyu rainfall forecasts over Zhejiang, China. Asia-Pac J Atmospheric Sci 58:265–280
Zhang N, Gao Z, Liu Y, Li D (2015) Sensitivity of a global climate model to the critical Richardson number in the boundary layer parameterization. J Geophys Res 120: 3310–3328

Editorial responsibility: Oliver Frauenfeld, College Station, Texas, USA
Reviewed by: 4 anonymous referees

Submitted: January 26, 2022
Accepted: November 16, 2022
Proofs received from author(s): December 20, 2022